SeMA Journal (2024) 81:51–80
https://doi.org/10.1007/s40324-023-00336-2

Parameter-robust preconditioners for Biot's model

Carmen Rodrigo[1] · Francisco J. Gaspar[1] · James Adler[2] · Xiaozhe Hu[2] · Peter Ohm[3] · Ludmil Zikatanov[4]

Received: 15 April 2023 / Accepted: 19 July 2023 / Published online: 5 August 2023

Abstract
This work presents an overview of the most relevant results obtained by the authors regarding the numerical solution of the Biot's consolidation problem by preconditioning techniques. The emphasis here is on the design of parameter-robust preconditioners for the efficient solution of the algebraic system of equations resulting after proper discretization of such poroelastic problems. The classical two- and three-field formulations of the problem are considered, and block preconditioners are presented for some of the discretization schemes that have been proposed by the authors for these formulations. These discretizations have been proved to be well-posed with respect to the physical and discretization parameters, what provides a framework to develop preconditioners that are robust with respect to such parameters as well. In particular, we construct both norm-equivalent (block diagonal) and field-of-value-equivalent (block triangular) preconditioners, which are proved to be parameter-robust. The theoretical results on this parameter-robustness are demonstrated by considering typical benchmark problems in the literature for Biot's model.

✉ Carmen Rodrigo
carmenr@unizar.es

Francisco J. Gaspar
fjgaspar@unizar.es

James Adler
James.Adler@tufts.edu

Xiaozhe Hu
xiaozhe.hu@tufts.edu

Peter Ohm
peter.ohm@riken.jp

Ludmil Zikatanov
ludmil@psu.edu

[1] Department of Applied Mathematics, University of Zaragoza, Pedro Cerbuna, 12, 50009 Zaragoza, Zaragoza, Spain

[2] Department of Mathematics, Tufts University, 177 College Avenue, Medford, MA 02155, USA

[3] Department of Mathematics, RIKEN Center for Computational Science, 7-1-26 Minatojima-minamimachi, Chuo-ku, Kobe, Hyogo 650-0047, Japan

[4] Department of Mathematics, The Pennsylvania State University, 107 McAllister Building, University Park, State College, PA 16802, USA

Keywords Biot's model · Poroelasticity · Well-posedness · Preconditioning · Parameter-robust preconditioners

Mathematics Subject Classification 65F08 · 65F10 · 65N12 · 65N22 · 65N30

1 Introduction

Coupling of fluid flow and mechanical deformation within a porous media is an important multi-physics problem appearing in many applications in several branches of technology and natural sciences. Such coupling was already modeled in the early one-dimensional work of Terzaghi [1], whereas the general three-dimensional mathematical formulation was established by Maurice Biot in several pioneering publications (see [2, 3]). Nowadays, geothermal energy extraction, CO2 storage, hydraulic fracturing or cancer research are among typical societal relevant applications of this model. In particular, here we consider the quasi–static Biot's model for soil consolidation, assuming the porous medium to be linearly elastic, homogeneous, isotropic, and saturated by a Newtonian fluid. According to Biot's theory [2], the consolidation process satisfies a system of partial differential equations (PDEs) which combines the equations for fluid flow and the elastic deformation of the solid matrix. If we consider a bounded open subset $\Omega \subset \mathbb{R}^d$, $d = 2, 3$ with regular boundary Γ, the governing equations are given as follows,

$$-\operatorname{div} \boldsymbol{\sigma}' + \alpha \nabla p = \rho \boldsymbol{g}, \quad \text{in } \Omega, \tag{1}$$

$$\frac{\partial}{\partial t}\left(\frac{1}{M_b} p + \alpha \operatorname{div} \boldsymbol{u}\right) + \operatorname{div} \boldsymbol{w} = f, \quad \text{in } \Omega. \tag{2}$$

Equation (1) corresponds to the equilibrium equation for the porous medium, which is given in terms of the effective stress $\boldsymbol{\sigma}'$, and where p is the pore pressure which is multiplied by the Biot–Willis constant α. The effective stress is related to the strain tensor $\boldsymbol{\epsilon}$ by the constitutive equation $\boldsymbol{\sigma}' = 2\mu\boldsymbol{\varepsilon}(\boldsymbol{u}) + \lambda \operatorname{div}(\boldsymbol{u})\boldsymbol{I}$ being λ and μ the so-called Lamé coefficients, which can be computed in terms of the Young modulus, E, and the Poisson ratio, ν, as follows:

$$\lambda = \frac{E\nu}{(1-2\nu)(1+\nu)} \quad \text{and} \quad \mu = \frac{E}{1+2\nu}.$$

Under the assumptions considered here, the strain tensor can be written in terms of the displacement vector $\boldsymbol{u}$ as follows $\boldsymbol{\varepsilon}(\boldsymbol{u}) = \frac{1}{2}(\nabla \boldsymbol{u} + \nabla \boldsymbol{u}^t)$. Finally, the right-hand side in (1) is given as the vector-valued function $\boldsymbol{g}$, which represents the gravitational force, multiplied by the bulk density $\rho = \phi\rho_f + (1-\phi)\rho_s$, where ρ_s and ρ_f are the densities of solid and fluid phases and ϕ is the porosity.

The fluid mass conservation equation (2) is written in terms of the variation of fluid content, being M_b the bulk modulus whose inverse is called storage coefficient and is related to the compressibility of the fluid, and the percolation velocity of the fluid relative to the soil $\boldsymbol{w}$. The source term f represents a forced fluid extraction or injection process. Finally, Darcy's law relates the fluid's flux $\boldsymbol{w}$ to the fluid's pressure gradient as follows $\boldsymbol{w} = -\frac{1}{\mu_f}\boldsymbol{K}(\nabla p - \rho_f \boldsymbol{g})$, where $\boldsymbol{K}$ is the absolute permeability tensor of the porous medium and μ_f is the viscosity of the fluid.

All these equations can be combined to obtain different formulations of the poroelasticity problem, depending on which variables one is interested in. The most widely used are the two field formulation in which the main variables are the displacement vector and the fluid

pressure, and the classical three-field formulation which includes also Darcy velocity in order to guarantee fluid mass conservation. But, of course, there are other different formulations, for example the three-field formulation in which the solid pressure is included as third variable as a way to deal with low-compressible or incompressible materials, or the recently introduced three-field formulation with the total pressure [4] which is a weighted sum of fluid and solid pressures. In this work, we will focus on the classical two- and three-field formulations, but the techniques used here can be applied to any of the formulations of the problem.

As we can observe in the system of equations presented above, many physical parameters are involved in the model, whose values vary for different real application problems. In fact, it is important to note that the values of some of these parameters may differ over several orders of magnitude depending on the application under consideration. As an example, the permeability can typically range from 10^{-9} to 10^{-21} m^2 in geophysical applications [4, 5], whereas in biophysical applications such as in the modeling of soft tissue or bone, the values for this parameter can range from 10^{-14} to 10^{-16} m^2 [6–8]. Due to this fact, the design of discretization techniques and solution algorithms that behave well with respect to this variation of the parameters is a big challenge and it has received a lot of attention during the last years.

Although finite difference and finite volume methods have been considered for the discretization of Biot's model in the literature [9–12], here we focus on the application of finite element methods. Stable finite-element schemes have been developed for the different formulations of Biot's model. For the classical two-field formulation, Taylor–Hood elements which satisfy an appropriate inf-sup condition have been used [13–15], and also appropriate stabilization techniques have been proposed for unstable finite-element pairs, such as the combination of piecewise linear elements for both variables [16–18]. For the classical three-field formulation, a non-conforming stable discretization based on Crouzeix–Raviart elements for displacement, lowest order Raviart–Thomas–Nédélec elements for Darcy's velocity, and piecewise constants for the pressure was proposed in [19]. In [20] a stabilization by bubble functions was presented to obtain a parameter-robust version of a typically considered discretization based on piecewise linear elements for displacements, Raviart–Thomas for Darcy's velocity and piecewise constants for the pressure. Another parameter-independent approach can be found in [21], where mixed finite element discretizations that fulfills mass conservation strongly at a discrete level are considered. In addition, stable discretization schemes have been proposed for other formulations, as for example, for the three-field formulation including the total pressure [4, 22], or the four-field formulation considering stress tensor, fluid flux, displacement, and pore-pressure as main variables [23]. More recently, in [24] the authors deal with conservative discretizations of the four-field formulation of Biot's equations utilizing total pressure.

Typical discretizations of Biot's model yield a large-scale sparse linear system of equations that has to be solved at each time step. Such linear systems are usually ill-conditioned and difficult to solve in practice. In fact, the solution of these systems of equations constitutes the main bottleneck in the numerical simulation of coupled poromechanics problems, which is mandatory for real applications, and therefore the design of efficient and fast solvers for Biot's model has become increasingly popular. Due to the size and the properties of the resulting systems, the application of iterative solution techniques, instead of direct methods, is usual. In particular, for the poroelastic problems considered here, there are two typical solution approaches: iterative coupling methods and fully-coupled or monolithic methods. Whereas monolithic techniques solve the resulting linear system simultaneously for all the involved unknowns, iterative coupling methods [25, 26], in contrast, consist of a sequential approach in which either the fluid flow problem or the geomechanics part is solved first, followed by

the solution of the other system, repeating this process until a converged solution within a prescribed tolerance is obtained. These iterative coupling methods have the main advantage of being able to combine existing software for simulating fluid flow and geomechanics in order to obtain the solution for the coupled problem. For this reason, the analysis and application of this type of schemes have received a lot of attention [27–31]. In particular, in [32, 33] a re-interpretation of the four commonly used sequential splitting methods as preconditioned-Richardson iterations with block-triangular preconditioning is presented, and such analysis indicates that a fully-implicit method outperforms the convergence rate of the sequential-implicit methods. In the context of monolithic methods, one can develop efficient preconditioners to accelerate the convergence of Krylov subspace methods or to design special smoothers within a multigrid framework. Examples of this latter approach can be found in [34–38], whereas the design of preconditioners for poromechanics has been addressed, for example, in [4, 9, 39–44], where many of the developed techniques are based on the Schur complement approach. More recently, the focus of this latter approach has been on the design of parameter-robust preconditioners [4, 45–48].

Thus, in this work we want to present some of the results obtained by the authors within this context. In particular, we address the construction of preconditioners for Biot's model, which are robust with respect to typical scales in material constants spanning over many orders of magnitude. This is done for different finite element discretizations of the two classical formulations of Biot's model, namely the displacement–pressure two-field formulation and the three-field formulation including the Darcy's velocity. For the first one, stabilized finite element pairs proposed and analyzed by the authors in [16, 17] are considered. For the three-field formulation, we propose preconditioners for two different discretizations: the nonconforming scheme given in [19] which is based on Crouzeix–Raviart finite elements for the displacements, lowest order Raviart–Thomas–Nédélec elements for the Darcy velocity, and piecewise constant approximation for the pressure, and the conforming stabilized scheme proposed in [20] which assumes piecewise linear elements for displacements, Raviart–Thomas finite elements for Darcy's velocity and piecewise constants for the pressure. With this purpose, we develop robust block preconditioners (e.g. [49, 50]) to accelerate the convergence of Krylov subspace methods. These preconditioners take advantage of the block structure of the discrete problem, decoupling the different fields at the preconditioning stage. Such block preconditioning is primarily attractive due to its simplicity, which allows us to focus on the character of the diagonal blocks, and to leverage extensive work on solving simpler problems. For example, algebraic multigrid [51] or auxiliary space decomposition methods [52, 53] can be considered for efficiently solving such blocks. Since the considered discretizations upon we build the preconditioners are well-posed with respect to the physical and discretization parameters, we are able to develop robust block preconditioners that efficiently solve the linear systems, independently of such parameters as well. Following the general framework developed in [33, 43, 46, 54, 55], we first consider block diagonal preconditioners (also known as norm-equivalent preconditioners). Then, we discuss block triangular (upper and lower) preconditioners following the framework developed in [54, 56, 57] for Field-of-Value (FOV) equivalent preconditioners. For both cases, we show that the theoretical bounds on their performance remain independent of the discretization and physical parameters of the problem.

We present theoretical results that guarantee the parameter robustness of the proposed preconditioners, but also we present appropriate numerical experiments to illustrate their robust performance. In particular, we will consider typical benchmark problems that are used in the literature to analyze the behavior of numerical methods for poromechanics. All these test problems were implemented in the HAZmath library [58], developed by some

of the authors, which contains routines for finite elements, multilevel solvers, and graph algorithms. The numerical tests were performed on a workstation with an 8-core 3 GHz Intel Xeon "Sandy Bridge" CPU and 32 GB of RAM per core.

The rest of the paper is organized as follows. Section 2 presents the general theory in which is based the design of the proposed block preconditioners. Next, Sect. 3 is divided into Sects. 3.1 and 3.2 which focus on the two- and three-field formulations of Biot's model, respectively. Section 3.1 is composed of four parts: first the formulation of the problem is presented, followed for two subsections with the proposed block diagonal and block triangular preconditioners respectively, and last a numerical experiment showing the performance of the proposed solvers for a benchmark problem in the literature. Section 3.2 first introduces the considered three-field formulation, and then it is divided into Sects. 3.2.1 and 3.2.2, dealing with two different discretizations for such a formulation, and whose structure is the same as that of Sect. 3.1. Finally, concluding remarks are made in Sect. 4.

2 Block preconditioning

Our aim is to derive uniform block preconditioners for the Biot's model based on the well-posedness of the considered discretizations. In order to do this, we will follow the general theory presented in [54, 55], and both block diagonal and triangular preconditioners will be developed. In the following, we introduce the general framework in which we will construct such preconditioners.

Let $\boldsymbol{X}$ be a real, separable Hilbert space equipped the inner product $(\cdot,\cdot)_{\boldsymbol{X}}$, which induces the norm $\|\cdot\|_{\boldsymbol{X}}$. Let us denote $\boldsymbol{X}'$ as a dual space to $\boldsymbol{X}$, being $\langle\cdot,\cdot\rangle$ the duality pairing between them. Then, we can consider an operator $\mathcal{A}:\boldsymbol{X}\mapsto\boldsymbol{X}'$ induced by a symmetric and bounded bilinear form $\mathcal{L}(\cdot,\cdot)$, that is, $\langle\mathcal{A}\boldsymbol{x},\boldsymbol{y}\rangle=\mathcal{L}(\boldsymbol{x},\boldsymbol{y})$. We assume that such a bilinear form satisfies the following continuity and inf-sup conditions:

$$|\mathcal{L}(\boldsymbol{x},\boldsymbol{y})|\leq\beta\|\boldsymbol{x}\|_{\boldsymbol{X}}\|\boldsymbol{y}\|_{\boldsymbol{X}},\ \forall\boldsymbol{x},\boldsymbol{y}\in\boldsymbol{X}, \tag{3}$$

$$\inf_{\boldsymbol{x}\in\boldsymbol{X}}\sup_{\boldsymbol{y}\in\boldsymbol{X}}\frac{\mathcal{L}(\boldsymbol{x},\boldsymbol{y})}{\|\boldsymbol{x}\|_{\boldsymbol{X}}\|\boldsymbol{y}\|_{\boldsymbol{X}}}\geq\gamma, \tag{4}$$

where $\beta,\gamma>0$. The properties of the bilinear form ensure that $\mathcal{A}$ is a bounded and symmetric operator and that the arising system of equations $\mathcal{A}\boldsymbol{x}=\boldsymbol{b}$ is well-posed. A competitive way for solving such a system of equations is to employ an iterative method coupled with a preconditioning technique. More precisely, we look for a preconditioner $\mathcal{M}$ such that $\mathcal{M}\mathcal{A}\boldsymbol{x}=\mathcal{M}\boldsymbol{b}$ or $\mathcal{A}\mathcal{M}\widehat{\boldsymbol{x}}=\boldsymbol{b}$ ($\widehat{\boldsymbol{x}}=\mathcal{M}^{-1}\boldsymbol{x}$) can be solved in a number of iterations independent of the system's size. We can manage this by choosing a preconditioning matrix which is equivalent to the system matrix in some sense. Thus, in the next subsections we will consider norm and field-of-values equivalence of matrices, which will provide us convergence bounds for Krylov subspace methods such as the Minimum Residual method (MINRES) or the Generalized Minimum Residual method (GMRES). In addition, if such equivalences hold independently of the parameters involved in the problem, we will obtain a robust convergence with respect to such parameters. With these assumptions, we will be able to design block diagonal and block triangular parameter-robust preconditioners for solving system $\mathcal{A}\boldsymbol{x}=\boldsymbol{b}$.

2.1 Norm-equivalent preconditioner

Let $\mathcal{M} : \boldsymbol{X}' \mapsto \boldsymbol{X}$ be a symmetric positive definite (SPD) operator, which induces an inner product $(\boldsymbol{x}, \boldsymbol{y})_{\mathcal{M}^{-1}} := \langle \mathcal{M}^{-1}\boldsymbol{x}, \boldsymbol{y}\rangle$ on $\boldsymbol{X}$ and the corresponding norm $\|\boldsymbol{x}\|^2_{\mathcal{M}^{-1}} := (\boldsymbol{x}, \boldsymbol{x})_{\mathcal{M}^{-1}}$. Since $\mathcal{M}\mathcal{A} : \boldsymbol{X} \mapsto \boldsymbol{X}$ is symmetric with respect to $(\cdot, \cdot)_{\mathcal{M}^{-1}}$, we can use $\mathcal{M}$ as preconditioner for the MINRES algorithm, and it is well-known [59] that the convergence rate of the preconditioned MINRES satisfies that

$$\|\mathcal{A}(\boldsymbol{x} - \boldsymbol{x}^m)\|_{\mathcal{M}} \leq 2\rho^m \|\mathcal{A}(\boldsymbol{x} - \boldsymbol{x}^0)\|_{\mathcal{M}}, \quad \text{with} \quad \rho = \frac{\kappa(\mathcal{M}\mathcal{A}) - 1}{\kappa(\mathcal{M}\mathcal{A}) + 1}, \tag{5}$$

being $\boldsymbol{x}^m$ the m-th iteration of the preconditioned MINRES, $\boldsymbol{x}$ the exact solution, and $\kappa(\mathcal{M}\mathcal{A})$ denotes the condition number of $\mathcal{M}\mathcal{A}$. Then, we are interested in estimating the condition number $\kappa(\mathcal{M}\mathcal{A})$ in order to know about the behavior of preconditioner $\mathcal{M}$.

Mardal and Winther [55] showed that, if the well-posedness conditions (3)–(4) hold, and $\mathcal{M}$ satisfies

$$c_1\|\boldsymbol{x}\|^2_{\boldsymbol{X}} \leq \|\boldsymbol{x}\|^2_{\mathcal{M}^{-1}} \leq c_2\|\boldsymbol{x}\|^2_{\boldsymbol{X}}, \tag{6}$$

then, $\mathcal{A}$ and $\mathcal{M}$ are *norm-equivalent* and we have the following bound for the condition number $\kappa(\mathcal{M}\mathcal{A}) \leq \frac{c_2\beta}{c_1\gamma}$.

This implies that the convergence rate of the MINRES method preconditioned with $\mathcal{M}$ satisfies $\rho \leq \frac{c_2\beta - c_1\gamma}{c_2\beta + c_1\gamma}$, and therefore, if the original problem is well-posed and the norm-equivalent inequality (6) is satisfied with constants c_1 and c_2 independent of the physical and discretization parameters, then the convergence rate of preconditioned MINRES is uniform, and $\mathcal{M}$ is a parameter-robust preconditioner. Later we will use this approach to design norm-equivalent preconditioners for the Biot's model and, as we will see, this will lead to block diagonal preconditioners.

In practice, a natural choice of norm-equivalent preconditioner is the Riesz operator $\mathcal{B} : \boldsymbol{X}' \mapsto \boldsymbol{X}$ corresponding to the inner product $(\cdot, \cdot)_{\boldsymbol{X}}$, that is,

$$(\mathcal{B}\boldsymbol{f}, \boldsymbol{x})_{\boldsymbol{X}} = \langle \boldsymbol{f}, \boldsymbol{x}\rangle, \quad \forall \boldsymbol{f} \in \boldsymbol{X}', \ \boldsymbol{x} \in \boldsymbol{X}. \tag{7}$$

It can be easily seen that $\mathcal{B}$ satisfies the norm-equivalent inequality (6) with constants c_1 and c_2 equal to one, and then $\kappa(\mathcal{B}\mathcal{A}) \leq \frac{\beta}{\gamma}$. Thus, if the well-posedness constants β and γ are independent on the physical and discretization parameters, $\mathcal{B}$ will provide a robust preconditioner.

2.2 FOV-equivalent preconditioner

In this section, we study a more general class of preconditioners as the field-of-values-equivalent (*FOV-equivalent*) preconditioners are. Let us consider a general operator $\mathcal{M}_L : \boldsymbol{X}' \mapsto \boldsymbol{X}$. $\mathcal{M}_L$ and $\mathcal{A}$ are said to be *FOV-equivalent* if there exist constants Σ and Υ such that, for any $\boldsymbol{x} \in \boldsymbol{X}$,

$$\Sigma \leq \frac{(\mathcal{M}_L\mathcal{A}\boldsymbol{x}, \boldsymbol{x})_{\mathcal{M}^{-1}}}{(\boldsymbol{x}, \boldsymbol{x})_{\mathcal{M}^{-1}}}, \quad \frac{\|\mathcal{M}_L\mathcal{A}\boldsymbol{x}\|_{\mathcal{M}^{-1}}}{\|\boldsymbol{x}\|_{\mathcal{M}^{-1}}} \leq \Upsilon. \tag{8}$$

In general, $\mathcal{M} : X' \to X$ can be any SPD operator, but we will consider $\mathcal{M}$ to be a SPD norm-equivalent preconditioner, and Σ and Υ are positive constants such that $\Sigma \leq \Upsilon$.
Such an operator $\mathcal{M}_L$ can be used as a preconditioner for the Generalized Minimum Residual

(GMRES) algorithm, in the way that, from [60, 61], the convergence rate of the preconditioned GMRES method is given by

$$\|\mathcal{M}_L\mathcal{A}(\boldsymbol{x}-\boldsymbol{x}^m)\|^2_{\mathcal{M}^{-1}} \leq \left(1-\frac{\Sigma^2}{\Upsilon^2}\right)^m \|\mathcal{M}_L\mathcal{A}(\boldsymbol{x}-\boldsymbol{x}^0)\|^2_{\mathcal{M}^{-1}}, \tag{9}$$

where $\boldsymbol{x}^m$ is the m-th iteration of the GMRES method preconditioned with $\mathcal{M}_L$ and $\boldsymbol{x}$ is the exact solution.

If constants Σ and Υ are independent of the physical and discretization parameters, then $\mathcal{M}_L$ is a uniform left preconditioner for GMRES and is referred to as an *FOV-equivalent* preconditioner. This approach leads to block lower triangular preconditioners.

Similar arguments also apply to right preconditioners for GMRES, so that $\mathcal{M}_U : \boldsymbol{X}' \mapsto \boldsymbol{X}$ and $\mathcal{A}$, are FOV equivalent if, for any $\boldsymbol{x}' \in \boldsymbol{X}'$,

$$\Sigma \leq \frac{(\mathcal{A}\mathcal{M}_U\boldsymbol{x}', \boldsymbol{x}')_{\mathcal{M}}}{(\boldsymbol{x}', \boldsymbol{x}')_{\mathcal{M}}}, \quad \frac{\|\mathcal{A}\mathcal{M}_U\boldsymbol{x}'\|_{\mathcal{M}}}{\|\boldsymbol{x}'\|_{\mathcal{M}}} \leq \Upsilon. \tag{10}$$

In this case, if Σ and Υ are independent of the physical and discretization parameters, $\mathcal{M}_U$ is a uniform right preconditioner for GMRES. Such an approach leads to block upper triangular preconditioners.

Naturally, FOV-equivalent preconditioners can be built based on the Riesz operator and the FOV-equivalence which can be derived from the well-posedness conditions (3)–(4), as done for example in [54].

In the next section, we apply the theoretical framework presented here to design appropriate block preconditioners for the chosen discretizations of Biot's model. We have to take into account that proper weighted norms have to be chosen so that the well-posedness constants are robust with respect to the physical and discretization parameters and thus the preconditioners also maintain this robustness property.

3 Parameter-robust preconditioners for Biot's model

3.1 Two-field formulation

First, we deal with the classical two-field formulation of Biot's model (1)–(2), where the main unknowns are the displacement vector $\boldsymbol{u}$ and the pore pressure p.

Let $L^2(\Omega)$ be the Hilbert space of square integrable scalar-valued functions defined on Ω, and let $H^1(\Omega)$ denote the space of square integrable scalar-valued functions whose first derivatives are in $L^2(\Omega)$, and $\boldsymbol{H}^1(\Omega)$ its vector counterpart. We consider appropriate Sobolev spaces $\boldsymbol{V} \subset \boldsymbol{H}^1(\Omega)$ and $Q \subset H^1(\Omega)$, which would include the information about the imposed boundary conditions, and by applying integration by parts, we obtain the following variational form:

For each $t \in (0, T]$, find $(\boldsymbol{u}(t), p(t)) \in \boldsymbol{V} \times Q$, such that

$$a(\boldsymbol{u}, \boldsymbol{v}) - \alpha(\operatorname{div} \boldsymbol{v}, p) = (\rho \boldsymbol{g}, \boldsymbol{v}), \quad \forall \boldsymbol{v} \in \boldsymbol{V}, \tag{11}$$

$$-\frac{1}{M_b}\left(\frac{\partial p}{\partial t} q\right) - \alpha\left(\operatorname{div}\frac{\partial \boldsymbol{u}}{\partial t}, q\right) - a_p(p, q) = (f, q), \quad \forall q \in Q, \tag{12}$$

where bilinear forms $a(\cdot,\cdot)$ and $a_p(\cdot,\cdot)$ are given as follows:

$$a(\boldsymbol{u}, \boldsymbol{v}) = 2\mu \int_\Omega \varepsilon(\boldsymbol{u}) : \varepsilon(\boldsymbol{v}) + \lambda \int_\Omega \operatorname{div} \boldsymbol{u} \operatorname{div} \boldsymbol{v},$$

$$a_p(p,q) = \int_\Omega \frac{\boldsymbol{K}}{\mu_f} \nabla p \cdot \nabla q,$$

$(\cdot,\cdot)$ denotes the standard inner product on $L^2(\Omega)$, and the problem is completed with suitable initial conditions.

In the rest of the section, we neglect the first term in the flow equation, assuming that the fluid is incompressible, since this results in the most challenging case.

Discretization

In order to introduce the finite element spatial discretization, we consider finite dimensional spaces $\boldsymbol{V}_h \subset \boldsymbol{V}$ and $Q_h \subset Q$. In particular, here we consider two stabilized discretizations for the two-field formulation of Biot's model proposed in [16, 17]. For the first one, $\boldsymbol{V}_h = \boldsymbol{V}_l$ is the space of piece-wise (with respect to a triangulation $\mathcal{T}_h$) linear continuous vector-valued functions on Ω and Q_h consists of piece-wise linear continuous scalar valued functions. This finite element pair is referred as the $\mathbb{P}_1$-$\mathbb{P}_1$ scheme. The second considered discretization is the so-called MINI element, introduced in [62], where Q_h is as before and $\boldsymbol{V}_h = \boldsymbol{V}_l \oplus \boldsymbol{V}_b$, being $\boldsymbol{V}_b$ the so-called space of bubble functions defined as

$$\boldsymbol{V}_b = \text{span}\{\varphi_{b,T} e_1, \ldots, \varphi_{b,T} e_d\}_{T\in\mathcal{T}_h}, \quad \varphi_{b,T} = \alpha_T \lambda_{1,T} \ldots \lambda_{d+1,T},$$

where $\lambda_{m,T}$ are the barycentric coordinates on T, e_j are the canonical Euclidean basis vectors in $\mathbb{R}^d$ and α_T is a normalizing constant for $\varphi_{b,T}$. Both finite element pairs have to be stabilized. The $\mathbb{P}_1$–$\mathbb{P}_1$ scheme needs a stabilization term to satisfy a uniform inf-sup condition, whereas both discretizations need such an stabilization for eliminating non-physical oscillations of the pressure approximation seen in practice [16]. Taking this into account, and using an implicit Euler scheme for time discretization on a time interval $(0, t_{max}]$ with constant time-step size τ, the fully discretized scheme at time t_n, $n = 1, 2, \ldots$ is as follows:
Find $\boldsymbol{u}_h^n \in \boldsymbol{V_h}$ and $p_h^n \in Q_h$, such that,

$$a(\boldsymbol{u}_h^n, \boldsymbol{v}_h) - \alpha(\text{div}\, \boldsymbol{v}_h, p_h^n) = (\boldsymbol{g}(t_n), \boldsymbol{v}_h), \quad \forall \boldsymbol{v}_h \in \boldsymbol{V}_h, \tag{13}$$

$$-\alpha(\text{div}\, \bar{\partial}_t \boldsymbol{u}_h^n, q_h) - a_p(p_h^n, q_h) - \eta h^2 (\nabla \bar{\partial}_t p_h^n, \nabla q_h) = (f(t_n), q_h), \quad \forall q_h \in Q_h, \tag{14}$$

where $\bar{\partial}_t \boldsymbol{u}_h^n := (\boldsymbol{u}_h^n - \boldsymbol{u}_h^{n-1})/\tau$, $\bar{\partial}_t p_h^n := (p_h^n - p_h^{n-1})/\tau$, and η represents the stabilization parameter.

At each time step, the resulting discrete problem can be written as the following two-by-two block linear system:

$$\mathcal{A}\boldsymbol{x} = \boldsymbol{b}, \quad \mathcal{A} = \begin{pmatrix} A_{\boldsymbol{u}} & \alpha B^T \\ \alpha B & -\tau A_p - \eta h^2 L_p \end{pmatrix}, \ \boldsymbol{x} = \begin{pmatrix} \boldsymbol{u} \\ p \end{pmatrix}, \text{ and } \boldsymbol{b} = \begin{pmatrix} \boldsymbol{f}_{\boldsymbol{u}} \\ f_p \end{pmatrix}, \tag{15}$$

where $a(\boldsymbol{u}, \boldsymbol{v}) \to A_{\boldsymbol{u}}$, $-(\text{div}\, \boldsymbol{u}, q) \to B$, $a_p(p,q) \to A_p$, and $(\nabla p, \nabla q) \to L_p$ represent the discrete versions of the variational forms.

Our target is to design block diagonal and triangular preconditioners for the solution of this discrete problem. In order to do that, as previously mentioned, we follow the framework proposed in [54, 55], which is based on the well-posedness of the discretized linear system at each time step. This well-posedness was already proved in [17]. In order to obtain parameter-robust preconditioners, however, we need to prove this well-posedness of the linear system (15), making special emphasis on the independence of the constant arising from the analysis with respect to any physical and discretization parameters.

With this purpose, the key is to define a proper weighted norm on $\boldsymbol{X} = \boldsymbol{V}_h \times Q_h$ as follows. For $\boldsymbol{x} = (\boldsymbol{u}, p)^T$, let us define,

$$\|\boldsymbol{x}\|_{\boldsymbol{X}}^2 := \|\boldsymbol{u}\|_{A_{\boldsymbol{u}}}^2 + \tau\|p\|_{A_p}^2 + \eta h^2\|p\|_{L_p}^2 + \frac{\alpha^2}{\zeta^2}\|p\|^2, \tag{16}$$

where $\|\boldsymbol{u}\|_{A_{\boldsymbol{u}}}^2 := a(\boldsymbol{u}, \boldsymbol{u})$, $\|p\|_{A_p}^2 := a_p(p, p)$, $\|p\|_{L_p}^2 := (\nabla p, \nabla p)$, $\zeta = \sqrt{\lambda + \frac{2\mu}{d}}$, $\|\cdot\|$ is the standard L^2-norm, and $d = 2$ or 3 is the dimension of the problem.
Next, we define the following composite bilinear form,

$$\mathcal{L}(\boldsymbol{x}, \boldsymbol{y}) = (A_{\boldsymbol{u}}\boldsymbol{u}, \boldsymbol{v}) + \alpha(B\boldsymbol{v}, p) + \alpha(B\boldsymbol{u}, q) - \tau(\mu_f^{-1}\mathbf{K}\nabla p, \nabla q) - \eta h^2(\nabla p, \nabla q), \tag{17}$$

for $\boldsymbol{x} = (\boldsymbol{u}, p)$ and $\boldsymbol{y} = (\boldsymbol{v}, q)$, and the well-posedness of problem (13)–(14) is demonstrated by the following theorem.

Theorem 1 *The bilinear form $\mathcal{L}(\boldsymbol{x}, \boldsymbol{y})$ given in (17) satisfies the continuity and inf-sup conditions (3)–(4) with constants γ and β independent of the physical and discretization parameters, and $\mathcal{A}$ defined in (15) is therefore an isomorphism from $\boldsymbol{X}$ to $\boldsymbol{X}'$ provided that the stabilization parameter, η, satisfies $\eta = \delta\frac{\alpha^2}{\zeta^2}$ with $\delta > 0$.*

Proof Due to our choice of finite element spaces $\boldsymbol{X} = \boldsymbol{V}_h \times Q_h$, we have the following inf-sup condition (see [63]),

$$\sup_{\boldsymbol{v}\in\boldsymbol{V}_h} \frac{(\operatorname{div}\boldsymbol{v}, q)}{\|\boldsymbol{v}\|_1} \geq \gamma_B^0\|q\| - \xi^0 h\|\nabla q\|, \quad \forall q \in Q_h, \tag{18}$$

where $\gamma_B^0 > 0$ and $\xi^0 \geq 0$ are constants that do not depend on the mesh size (notice that if we use the MINI element, then $\xi^0 = 0$). From the definition of ζ, it holds that $\|\boldsymbol{v}\|_{A_{\boldsymbol{u}}} \leq \sqrt{d}\zeta\|\boldsymbol{v}\|_1$, and therefore we can reformulate the inf-sup condition, (18), as follows,

$$\sup_{\boldsymbol{v}\in\boldsymbol{V}_h} \frac{(B\boldsymbol{v}, q)}{\|\boldsymbol{v}\|_{A_{\boldsymbol{u}}}} \geq \sup_{\boldsymbol{v}\in\boldsymbol{V}_h} \frac{(B\boldsymbol{v}, q)}{\sqrt{d}\zeta\|\boldsymbol{v}\|_1} \geq \frac{\gamma_B^0}{\sqrt{d}\zeta}\|q\| - \frac{\xi^0}{\sqrt{d}\zeta}h\|\nabla q\| =: \frac{\gamma_B}{\zeta}\|q\| - \frac{\xi}{\zeta}h\|\nabla q\|, \tag{19}$$

where $\gamma_B := \gamma_B^0/\sqrt{d}$ and $\xi = \xi^0/\sqrt{d}$.

Based on the inf-sup conditions (18) and (19), for any p, there exists $\boldsymbol{w} \in \boldsymbol{V}_h$ such that $(B\boldsymbol{w}, p) \geq \left(\frac{\gamma_B}{\zeta}\|p\| - \frac{\xi}{\zeta}h\|\nabla p\|\right)\|\boldsymbol{w}\|_{A_{\boldsymbol{u}}}$ and, without loss of generality, we may assume $\|\boldsymbol{w}\|_{A_{\boldsymbol{u}}} = \|p\|$, and then we have,

$$(B\boldsymbol{w}, p) \geq \left(\frac{\gamma_B}{\zeta}\|p\| - \frac{\xi}{\zeta}h\|\nabla p\|\right)\|p\|. \tag{20}$$

For a given pair $(\boldsymbol{u}, p) \in \boldsymbol{V}_h \times Q_h$ and $\boldsymbol{w}$ defined as above, we choose $\boldsymbol{v} = \boldsymbol{u} + \theta\boldsymbol{w}, \theta = \vartheta\frac{\gamma_B\alpha}{\zeta}$ and $q = -p$ and using the facts above, we have,

$$\begin{aligned}\mathcal{L}(\boldsymbol{x}, \boldsymbol{y}) &= (A_{\boldsymbol{u}}\boldsymbol{u}, \boldsymbol{u}+\theta\boldsymbol{w}) + \alpha(B(\boldsymbol{u}+\theta\boldsymbol{w}), p) - \alpha(B\boldsymbol{u}, p) + \tau(K\nabla p, \nabla p) + \eta h^2(\nabla p, \nabla p)\\ &\geq \|\boldsymbol{u}\|_{A_{\boldsymbol{u}}}^2 - \vartheta\|\boldsymbol{u}\|_{A_{\boldsymbol{u}}}\frac{\gamma_B\alpha}{\zeta}\|p\| + \vartheta\frac{\gamma_B^2\alpha^2}{\zeta^2}\|p\|^2 - \vartheta\frac{\gamma_B\alpha^2}{\zeta^2}\xi h\|\nabla p\|\|p\|\\ &\quad + \tau\|p\|_{A_p}^2 + \frac{\delta}{\xi^2}\frac{\alpha^2}{\zeta^2}\xi^2 h^2\|\nabla p\|^2\end{aligned}$$

$$\geq \begin{pmatrix} \|\boldsymbol{u}\|_{A_{\boldsymbol{u}}} \\ \frac{\gamma_B \alpha}{\zeta}\|p\| \\ \frac{\alpha}{\zeta}\xi h\|\nabla p\| \\ \sqrt{\tau}\|p\|_{A_p} \end{pmatrix}^T \begin{pmatrix} 1 & -\vartheta/2 & 0 & 0 \\ -\vartheta/2 & \vartheta & -\vartheta/2 & 0 \\ 0 & -\vartheta/2 & \delta/\xi^2 & 0 \\ 0 & 0 & 0 & 1 \end{pmatrix} \begin{pmatrix} \|\boldsymbol{u}\|_{A_{\boldsymbol{u}}} \\ \frac{\gamma_B \alpha}{\zeta}\|p\| \\ \frac{\alpha}{\zeta}\xi h\|\nabla p\| \\ \sqrt{\tau}\|p\|_{A_p} \end{pmatrix}.$$

If $0 < \vartheta < \min\{2, \frac{2\delta}{\xi^2}\}$, the matrix in the middle is SPD and there exists γ_0 such that

$$\mathcal{L}(\boldsymbol{x}, \boldsymbol{y}) \geq \gamma_0 \left(\|\boldsymbol{u}\|_{A_{\boldsymbol{u}}}^2 + \frac{\gamma_B^2 \alpha^2}{\zeta^2}\|p\|^2 + \frac{\alpha^2}{\zeta^2}\xi^2 h^2 \|\nabla p\|^2 + \tau \|p\|_{A_p}^2 \right) \geq \tilde{\gamma}\|\boldsymbol{x}\|_{\boldsymbol{X}}^2,$$

where $\tilde{\gamma} = \gamma_0 \min\{\gamma_B^2, \xi^2/\delta\}$. Since, it is straightforward to verify also that $\|(\boldsymbol{v}, q)\|_{\boldsymbol{X}}^2 \leq \bar{\gamma}^2 \|(\boldsymbol{u}, p)\|_{\boldsymbol{X}}^2$, then $\mathcal{L}$ satisfies the inf-sup condition (4) with $\gamma = \tilde{\gamma}/\bar{\gamma}$. The boundedness of $\mathcal{L}$, that is (3), is obtained by the continuity of each term and the Cauchy–Schwarz inequality. □

Norm-equivalent preconditioners

Once we have proved that the well-posedness condition (4) holds, we look for SPD operators that satisfy the norm-equivalence inequality (6). As mentioned in Sect. 2.1, one natural choice is the Riesz operator, which for the two-field stabilized discretization and the norm $\|\cdot\|_{\boldsymbol{X}}$ defined in (16) is given as follows:

$$\mathcal{B}_D = \begin{pmatrix} A_{\boldsymbol{u}} & 0 \\ 0 & \tau A_p + \eta h^2 L_p + \frac{\alpha^2}{\zeta^2} M \end{pmatrix}^{-1}, \tag{21}$$

where M is the mass matrix of the pressure block.

In practice, applying preconditioner $\mathcal{B}_D$ implies inverting the diagonal blocks exactly, which can be expensive and sometimes infeasible. Thus, we consider the following inexact preconditioner:

$$\widehat{\mathcal{B}}_D = \begin{pmatrix} S_{\boldsymbol{u}} & 0 \\ 0 & S_p \end{pmatrix},$$

where the diagonal blocks $S_{\boldsymbol{u}}$ and S_p are SPD and spectrally equivalent to the diagonal blocks in $\mathcal{B}_D$, that is,

$$c_{1,\boldsymbol{u}}(S_{\boldsymbol{u}}\boldsymbol{u}, \boldsymbol{u}) \leq (A_{\boldsymbol{u}}^{-1}\boldsymbol{u}, \boldsymbol{u}) \leq c_{2,\boldsymbol{u}}(S_{\boldsymbol{u}}\boldsymbol{u}, \boldsymbol{u}), \tag{22}$$

$$c_{1,p}(S_p p, p) \leq \left(\left(\tau A_p + \eta h^2 L_p + \frac{\alpha^2}{\zeta^2} M \right)^{-1} p, p \right) \leq c_{2,p}(S_p p, p), \tag{23}$$

being the involved constants independent of discretization and physical parameters.

$\widehat{\mathcal{B}}_D$ and $\mathcal{A}$ are norm-equivalent and we can estimate the condition number $\kappa(\widehat{\mathcal{B}}_D \mathcal{A}) = \mathcal{O}(1)$ by Theorem 1.

FOV-equivalent preconditioners

For a more general approach, we propose now block triangular preconditioners for the stabilized system given in (15), following the FOV-equivalent framework presented in Sect. 2.2. For simplicity in the analysis, we slightly modify the system matrix $\mathcal{A}$ by negating the second equation, but still denote it by $\mathcal{A}$.

First, we consider the following block lower triangular preconditioner:

$$\mathcal{B}_L = \begin{pmatrix} A_{\boldsymbol{u}} & 0 \\ -\alpha B & \tau A_p + \eta h^2 L_p + \frac{\alpha^2}{\zeta^2} M \end{pmatrix}^{-1}, \tag{24}$$

and we need to show that the FOV-equivalence in (8) is satisfied.

Theorem 2 *There exist constants Σ and Υ, independent of discretization or physical parameters, such that, for any $\boldsymbol{x} = (\boldsymbol{u}, p)^T \neq \boldsymbol{0}$,*

$$\Sigma \leq \frac{(\mathcal{B}_L \mathcal{A}\boldsymbol{x}, \boldsymbol{x})_{(\mathcal{B}_D)^{-1}}}{(\boldsymbol{x}, \boldsymbol{x})_{(\mathcal{B}_D)^{-1}}}, \ \frac{\|\mathcal{B}_L \mathcal{A}\boldsymbol{x}\|_{(\mathcal{B}_D)^{-1}}}{\|\boldsymbol{x}\|_{(\mathcal{B}_D)^{-1}}} \leq \Upsilon,$$

provided that $\eta = \delta \frac{\alpha^2}{\zeta^2}$ with $\delta > 0$.

Proof By direct computation first, and applying the reformulated inf-sup condition given in (19) secondly,

$$\begin{aligned}
(\mathcal{B}_L \mathcal{A}\boldsymbol{x}, \boldsymbol{x})_{(\mathcal{B}_D)^{-1}} &= (\boldsymbol{u}, \boldsymbol{u})_{A_{\boldsymbol{u}}} + \alpha(B^T p, \boldsymbol{u}) + \tau(p, p)_{A_p} \\
&\quad + \eta h^2 (L_p p, p) + \alpha^2 (B A_{\boldsymbol{u}}^{-1} B^T p, p) \\
&\geq \Sigma_0 \left(\|\boldsymbol{u}\|_{A_{\boldsymbol{u}}}^2 + \tau \|p\|_{A_p}^2 + \eta h^2 \|p\|_{L_p}^2 + \alpha^2 \|B^T p\|_{A_{\boldsymbol{u}}^{-1}}^2 \right) \\
&\geq \Sigma_0 \left[\|\boldsymbol{u}\|_{A_{\boldsymbol{u}}}^2 + \tau \|p\|_{A_p}^2 + \eta h^2 \|p\|_{L_p}^2 + \alpha^2 \left(\frac{\gamma_B}{\zeta} \|p\| - \frac{\xi}{\zeta} h \|\nabla p\| \right)^2 \right].
\end{aligned}$$

By choosing $\frac{1}{1+\delta/\xi^2} < \theta < 1$, and taking into account that $\eta = \delta \frac{\alpha^2}{\zeta^2}$ with $\delta > 0$, we can obtain the lower bound in the theorem:

$$\begin{aligned}
(\mathcal{B}_L \mathcal{A}\boldsymbol{x}, \boldsymbol{x})_{(\mathcal{B}_D)^{-1}} &\geq \Sigma_0 \left[\|\boldsymbol{u}\|_{A_{\boldsymbol{u}}}^2 + \tau \|p\|_{A_p}^2 \right. \\
&\quad \left. + (1-\theta) \frac{\gamma_B^2 \alpha^2}{\zeta^2} \|p\|^2 + \left(1 + \frac{\delta}{\xi^2} - \frac{1}{\theta} \right) \frac{\alpha^2}{\zeta^2} \xi^2 h^2 \|\nabla p\|^2 \right] \\
&\geq \Sigma_0 \Sigma_1 \left(\|\boldsymbol{u}\|_{A_{\boldsymbol{u}}}^2 + \tau \|p\|_{A_p}^2 + \eta h^2 \|p\|_{L_p}^2 + \frac{\alpha^2}{\zeta^2} \|p\|^2 \right) \\
&=: \Sigma (\boldsymbol{x}, \boldsymbol{x})_{(\mathcal{B}_D)^{-1}},
\end{aligned}$$

where $\Sigma_1 := \min\{1, (1-\theta)\gamma_B^2, \left(1 + \frac{\delta}{\xi^2} - \frac{1}{\theta}\right) \frac{\xi^2}{\delta}\}$. The upper bound Υ can be obtained directly from the continuity of each term, the Cauchy-Schwarz inequality, and the fact that $\|B^T p\|_{A_{\boldsymbol{u}}^{-1}} \leq \frac{1}{\zeta} \|p\|$. To show the last inequality we use the identity $\|z\|_{A_{\boldsymbol{u}}} = \frac{(y,z)_{A_{\boldsymbol{u}}}}{\|y\|_{A_{\boldsymbol{u}}}}$. We then have

$$\begin{aligned}
\|B^T p\|_{A_{\boldsymbol{u}}^{-1}} &= \sqrt{\left(A_{\boldsymbol{u}}^{-1} B^T p, B^T p \right)} = \sqrt{\left(A_{\boldsymbol{u}}^{-1} B^T p, A_{\boldsymbol{u}}^{-1} B^T p \right)_{A_{\boldsymbol{u}}}} \\
&= \|A_{\boldsymbol{u}}^{-1} B^T p\|_{A_{\boldsymbol{u}}} = \sup_{\boldsymbol{v}} \frac{\left(\boldsymbol{v}, A_{\boldsymbol{u}}^{-1} B^T p \right)_{A_{\boldsymbol{u}}}}{\|\boldsymbol{v}\|_{A_{\boldsymbol{u}}}} \\
&= \sup_{\boldsymbol{v}} \frac{(B\boldsymbol{v}, p)}{\|\boldsymbol{v}\|_{A_{\boldsymbol{u}}}} \leq \|p\| \sup_{\boldsymbol{v}} \frac{\|B\boldsymbol{v}\|_{L^2}}{\|\boldsymbol{v}\|_{A_{\boldsymbol{u}}}}.
\end{aligned} \tag{25}$$

Since by definition we have that $\|\boldsymbol{v}\|^2_{A_{\boldsymbol{u}}} = 2\mu\|\varepsilon(\boldsymbol{v})\|^2_{L^2} + \lambda\|B\boldsymbol{v}\|^2_{L^2}$ and also the spatial dimension satisfies $d \geq 1$, it is evident that

$$\begin{aligned}\frac{2\mu}{d}\|B\boldsymbol{v}\|^2_{L^2} &= \frac{2\mu}{d}\,\|\varepsilon_{11}(\boldsymbol{v}) + \cdots + \varepsilon_{dd}(\boldsymbol{v})\|^2_{L^2} \\ &\leq 2\mu\left(\|\varepsilon_{11}(\boldsymbol{v})\|^2_{L^2} + \cdots + \|\varepsilon_{dd}(\boldsymbol{v})\|^2_{L^2}\right) \leq 2\mu\,\|\varepsilon(\boldsymbol{v})\|^2_{L^2}\,.\end{aligned} \tag{26}$$

Therefore, we obtain

$$\begin{aligned}\zeta^2\|B\boldsymbol{v}\|^2_{L^2} &= \left(\frac{2\mu}{d} + \lambda\right)\|B\boldsymbol{v}\|^2_{L^2} \\ &\leq 2\mu\,\|\varepsilon(\boldsymbol{v})\|^2_{L^2} + \lambda\|B\boldsymbol{v}\|^2_{L^2} = \|\boldsymbol{v}\|^2_{A_{\boldsymbol{u}}}\,.\end{aligned} \tag{27}$$

Taking square root and a supremum over $\boldsymbol{v}$ shows that $\sup_{\boldsymbol{v}} \frac{\|B\boldsymbol{v}\|_{L^2}}{\|\boldsymbol{v}\|_{A_{\boldsymbol{u}}}} \leq \frac{1}{\zeta}$. □

The inexact counterpart of (24) is also considered,

$$\widehat{\mathcal{B}}_L = \begin{pmatrix} S_{\boldsymbol{u}}^{-1} & 0 \\ -\alpha B & S_p^{-1} \end{pmatrix}^{-1}, \tag{28}$$

where $S_{\boldsymbol{u}}$ and S_p satisfy the spectrally equivalences (22) and (23). Then, similarly, we can show that $\widehat{\mathcal{B}}_L$ is also FOV-equivalent with $\mathcal{A}$ and, therefore, it can be used as preconditioner for GMRES. Due to the fact that the proofs are similar, we only state the results here. The next theorem is easily seen to be analogous to [64, Theorem 4.4].

Theorem 3 *If $\|I - S_{\boldsymbol{u}}A_{\boldsymbol{u}}\|_{A_{\boldsymbol{u}}} \leq \rho$ with $0 \leq \rho < 1$, there exist constants Σ and Υ, independent of discretization and physical parameters, such that, for any $\boldsymbol{x} = (\boldsymbol{u}, p)^T \neq \boldsymbol{0}$, it holds that*

$$\Sigma \leq \frac{(\widehat{\mathcal{B}}_L\mathcal{A}\boldsymbol{x}, \boldsymbol{x})_{(\widehat{\mathcal{B}}_D)^{-1}}}{(\boldsymbol{x}, \boldsymbol{x})_{(\widehat{\mathcal{B}}_D)^{-1}}}, \quad \frac{\|\widehat{\mathcal{B}}_L\mathcal{A}\boldsymbol{x}\|_{(\widehat{\mathcal{B}}_D)^{-1}}}{\|\boldsymbol{x}\|_{(\widehat{\mathcal{B}}_D)^{-1}}} \leq \Upsilon,$$

provided that $\eta = \delta\frac{\alpha^2}{\zeta^2}$ with $\delta > 0$.

In a similar way, we can construct block upper triangular preconditioners, both exact and inexact versions,

$$\mathcal{B}_U = \begin{pmatrix} A_{\boldsymbol{u}} & \alpha B^T \\ 0 & \tau A_p + \eta h^2 L_p + \frac{\alpha^2}{\zeta^2} M \end{pmatrix}^{-1} \text{ and } \widehat{\mathcal{B}}_U = \begin{pmatrix} S_{\boldsymbol{u}}^{-1} & \alpha B^T \\ 0 & S_p^{-1} \end{pmatrix}^{-1}, \tag{29}$$

and we can prove the FOV-equivalence (10), so that they give rise to uniform right preconditioners for GMRES.

Numerical experiment: 3D footing problem

In order to demonstrate the robustness of the proposed preconditioners, we consider a classical benchmark in the literature, that is, a 3D footing problem (see for example [34]). The computational domain, depicted in the left side of Fig. 1, is a three dimensional cube $\Omega = (-32, 32) \times (-32, 32) \times (0, 64)$ that represents a block of porous soil, on which a uniform load of intensity 0.1 N/m^2 is applied in a square of size 32×32 m^2 at the middle of the top of the domain. The base of the domain is fixed in all directions, and the remaining boundary is considered to be stress free. A no-flow boundary condition is applied at the compression zone, and the remaining boundary is assumed to be free to drain.

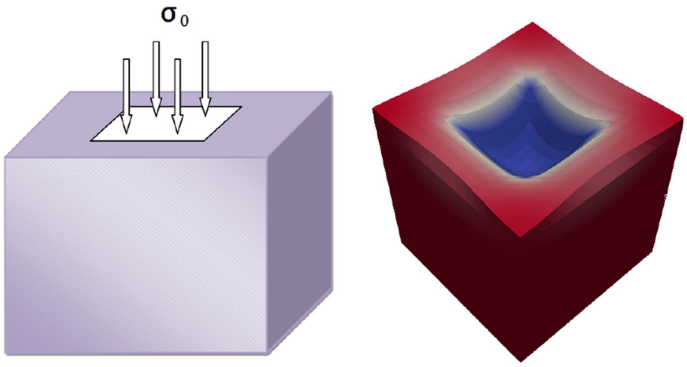

Fig. 1 Computational domain and boundary conditions on the left picture, and example of the deformation obtained after applying the uniform load on the right picture

For the simulations we consider the stabilized $\mathbb{P}_1$-$\mathbb{P}_1$ scheme, which has been implemented in the HAZmath library [58]. As an example of the solution of this benchmark, we show in the right side of Fig. 1 the deformation obtained after applying the uniform load.

Regarding the considered material properties, in this numerical experiment, we fix the Young's modulus $E = 3 \times 10^4$ N/m^2, whereas the Poisson's ratio ν and the permeability $\mathbf{K}$ will be varied in some of the experiments. We will consider a diagonal permeability tensor $\boldsymbol{K} = K\boldsymbol{I}$, with K constant.

We start by analyzing the performance of the proposed preconditioners with respect to the discretization parameters, so that we consider different values of the mesh size h and the time step size τ. In particular, h will vary from $1/4$ to $1/32$, whereas τ will range from 0.0001 to 0.1. The physical parameters are considered fixed as $K = 10^{-6}$ m^2 and $\nu = 0.2$.

We consider flexible GMRES as the outer iteration with a relative residual stopping criteria of 10^{-6}, which is preconditioned with the block diagonal and triangular proposed preconditioners $\mathcal{B}_D$, $\mathcal{B}_L$, $\mathcal{B}_U$, as well as, with their inexact counterparts $\widehat{\mathcal{B}}_D$, $\widehat{\mathcal{B}}_L$, $\widehat{\mathcal{B}}_U$. When these latter are considered, the diagonal blocks are solved inexactly by preconditioned GMRES with a tolerance of 10^{-2}. In Table 1, we show the number of GMRES iterations needed to fulfill the stopping criterion, and we can observe that the proposed preconditioners are robust with respect to the discretization parameters h and τ.

Next, we investigate the robustness of the block preconditioners with respect to the physical parameters K and ν. Thus, we fix the mesh size as $h = 1/16$ and the time step size as $\tau = 0.01$, and vary the values of the permeability K and the Poisson's ratio ν. In Table 2, we show the number of GMRES iterations needed to achieve the stopping criterion, for the different exact and inexact preconditioners. The results corresponding to the variation of the permeability are shown on the left part of the table, where K varies from 1 to 10^{-10} while ν is fixed as 0.2. On the right part of the table, we fix $K = 10^{-6}$ and we consider different values of ν from 0.1 to 0.499, which already is close to the incompressible material case. From the iteration counts in the table, we can see that the proposed preconditioners are also quite robust with respect to the physical parameters.

Table 1 Two-field stabilized $\mathbb{P}_1$-$\mathbb{P}_1$ scheme: iteration counts for the block preconditioners for different values of the discretization parameters ($*$ means the direct method for solving diagonal blocks is out of memory)

	$\mathcal{B}_D$				$\mathcal{B}_L$				$\mathcal{B}_U$			
τ/h	$\frac{1}{4}$	$\frac{1}{8}$	$\frac{1}{16}$	$\frac{1}{32}$	$\frac{1}{4}$	$\frac{1}{8}$	$\frac{1}{16}$	$\frac{1}{32}$	$\frac{1}{4}$	$\frac{1}{8}$	$\frac{1}{16}$	$\frac{1}{32}$
0.1	7	7	8	*	5	5	6	*	4	4	4	*
0.01	7	7	8	*	5	5	6	*	4	4	5	*
0.001	7	7	8	*	5	5	6	*	5	5	6	*
0.0001	7	7	8	*	5	5	6	*	5	5	6	*
	$\widehat{\mathcal{B}}_D$				$\widehat{\mathcal{B}}_L$				$\widehat{\mathcal{B}}_U$			
τ/h	$\frac{1}{4}$	$\frac{1}{8}$	$\frac{1}{16}$	$\frac{1}{32}$	$\frac{1}{4}$	$\frac{1}{8}$	$\frac{1}{16}$	$\frac{1}{32}$	$\frac{1}{4}$	$\frac{1}{8}$	$\frac{1}{16}$	$\frac{1}{32}$
0.1	8	8	9	9	6	6	8	8	6	6	8	8
0.01	8	8	9	9	6	6	8	8	6	6	8	8
0.001	8	8	9	9	6	6	8	8	6	6	8	8
0.0001	8	8	9	9	7	6	8	8	6	7	8	8

Table 2 Two-field stabilized $\mathbb{P}_1$-$\mathbb{P}_1$ scheme: iteration counts when varying physical parameters K or ν

	$\nu = 0.2$ and varying K						$K = 10^{-6}$ and varying ν					
	1	10^{-2}	10^{-4}	10^{-6}	10^{-8}	10^{-10}	0.1	0.2	0.4	0.45	0.49	0.499
$\mathcal{B}_D$	4	7	8	8	8	8	7	8	11	11	12	12
$\mathcal{B}_L$	2	5	6	6	6	6	5	6	8	8	8	9
$\mathcal{B}_U$	3	4	5	5	5	5	4	5	6	6	5	4
$\widehat{\mathcal{B}}_D$	5	8	9	9	9	9	8	9	12	13	14	13
$\widehat{\mathcal{B}}_L$	5	7	8	8	8	8	7	8	11	11	12	12
$\widehat{\mathcal{B}}_U$	5	7	8	8	9	8	7	8	7	8	17	11

3.2 Three-field formulation

In many of the applications where the coupling of fluid flow and mechanical deformation within a porous media is important, the flow of the fluid through the medium is of primary interest. Although from the reduced displacement–pressure formulation the fluid flux can be recovered, a natural approach is to introduce this value as a primary variable instead, so that we deal with the classical three-field formulation of the Biot's model. The incorporation of this extra unknown can be seen as a disadvantage against the two-field formulation, regarding the computational cost, but there appear other advantages of this approach. The direct calculation of the fluid flux, instead of its calculation by post-processing allows a higher order of accuracy in its computation, and in addition, the mass conservation for the fluid phase is ensured by using continuous elements for the fluid flux variable.

Since the three-field formulation considered here has the displacement $\boldsymbol{u}$, the pore pressure p and the Darcy's velocity $\boldsymbol{w}$ as primary unknowns, let us define proper Sobolev spaces $\boldsymbol{V} \subset \boldsymbol{H}^1(\Omega)$, $Q \subset H^1(\Omega)$ and $\boldsymbol{W} \subset \boldsymbol{H}(\mathrm{div}, \Omega)$, where $\boldsymbol{H}(\mathrm{div}, \Omega)$ contains the square integrable vector-valued functions with square integrable divergence. Then, the variational formulation for Biot's three-field consolidation model reads:

For each $t \in (0, T]$, find $(\boldsymbol{u}(t), p(t), \boldsymbol{w}(t)) \in \boldsymbol{V} \times Q \times \boldsymbol{W}$ such that

$$a(\boldsymbol{u}, \boldsymbol{v}) - \alpha(p, \mathrm{div}\, \boldsymbol{v}) = (\rho \boldsymbol{g}, \boldsymbol{v}), \quad \forall\, \boldsymbol{v} \in \boldsymbol{V}, \tag{30}$$

$$\frac{1}{M_b}\left(\frac{\partial p}{\partial t}, q\right) + \alpha\left(\operatorname{div}\frac{\partial \boldsymbol{u}}{\partial t}, q\right) + (\operatorname{div}\boldsymbol{w}, q) = (f, q), \quad \forall\, q \in Q, \tag{31}$$

$$(\boldsymbol{K}^{-1}\mu_f \boldsymbol{w}, \boldsymbol{r}) - (p, \operatorname{div}\boldsymbol{r}) = (\rho_f \boldsymbol{g}, \boldsymbol{r}), \quad \forall\, \boldsymbol{r} \in \boldsymbol{W}, \tag{32}$$

where $a(\boldsymbol{u}, \boldsymbol{v})$ corresponds to the bilinear form representing linear elasticity, already introduced in Sect. 3.1.

In order to consider the finite element approximation of problem (30)–(32), given a partition of the domain Ω into d-dimensional simplices, $\mathcal{T}_h$, we associate a triple of piecewise polynomial, finite-dimensional spaces,

$$\boldsymbol{V}_h \subset \boldsymbol{V}, \quad Q_h \subset Q, \quad \boldsymbol{W}_h \subset \boldsymbol{W}. \tag{33}$$

By using backward Euler as a time discretization on a time interval $(0, T]$ with constant time-step size τ, the discrete scheme corresponding to the three-field formulation (30)–(32) reads:

Find $(\boldsymbol{u}_h^m, p_h^m, \boldsymbol{w}_h^m) \in \boldsymbol{V}_h \times Q_h \times \boldsymbol{W}_h$ such that

$$a(\boldsymbol{u}_h^m, \boldsymbol{v}_h) - \alpha(p_h^m, \operatorname{div}\boldsymbol{v}_h) = (\rho\boldsymbol{g}, \boldsymbol{v}_h), \quad \forall\, \boldsymbol{v}_h \in \boldsymbol{V}_h, \tag{34}$$

$$\frac{1}{M_b}\left(p_h^m, q_h\right) + \alpha\left(\operatorname{div}\boldsymbol{u}_h^m, q_h\right) + \tau(\operatorname{div}\boldsymbol{w}_h^m, q_h) = (\widetilde{f}, q_h), \quad \forall\, q_h \in Q_h, \tag{35}$$

$$\tau(\boldsymbol{K}^{-1}\mu_f \boldsymbol{w}_h^m, \boldsymbol{r}_h) - \tau(p_h^m, \operatorname{div}\boldsymbol{r}_h) = \tau(\rho_f \boldsymbol{g}, \boldsymbol{r}_h), \quad \forall\, \boldsymbol{r}_h \in \boldsymbol{W}_h, \tag{36}$$

where $(\widetilde{f}, q_h) = \tau(f, q_h) + \frac{1}{M_b}\left(p_h^{m-1}, q_h\right) + \left(\alpha \operatorname{div}\boldsymbol{u}_h^{m-1}, q_h\right)$, and $(\boldsymbol{u}_h^m, p_h^m, \boldsymbol{w}_h^m)$ is an approximation to $(\boldsymbol{u}(\cdot, t_m), p(\cdot, t_m), \boldsymbol{w}(\cdot, t_m))$, at time $t_m = m\tau$, $m = 1, 2, \ldots$. Note that the last equation has been scaled by τ for symmetry.

Moreover, this discrete variational form can be represented in block matrix form,

$$\mathcal{A}\begin{pmatrix} \boldsymbol{u}_h \\ p_h \\ \boldsymbol{w}_h \end{pmatrix} = \boldsymbol{b}, \quad \text{with } \mathcal{A} = \begin{pmatrix} A_{\boldsymbol{u}} & \alpha B_{\boldsymbol{u}}^T & 0 \\ -\alpha B_{\boldsymbol{u}} & \frac{1}{M_b} M_p & -\tau B_{\boldsymbol{w}} \\ 0 & \tau B_{\boldsymbol{w}}^T & \tau M_{\boldsymbol{w}} \end{pmatrix}, \tag{37}$$

where $\boldsymbol{u}$, p, and $\boldsymbol{w}$ are the unknown vectors for the displacement, the pressure, and the Darcy velocity, respectively. The blocks in the definition of matrix $\mathcal{A}$ correspond to the following bilinear forms:

$$a(\boldsymbol{u}_h, \boldsymbol{v}_h) \to A_{\boldsymbol{u}}, \quad -(\operatorname{div}\boldsymbol{u}_h, q_h) \to B_{\boldsymbol{u}},$$
$$-(\operatorname{div}\boldsymbol{w}_h, q_h) \to B_{\boldsymbol{w}}, \quad (\boldsymbol{K}^{-1}\mu_f \boldsymbol{w}_h, \boldsymbol{r}_h) \to M_{\boldsymbol{w}}, \quad (p_h, q_h) \to M_p.$$

3.2.1 Stabilized $\mathbb{P}_1$–RT–$\mathbb{P}_0$

Due to its application to existing reservoir engineering simulators, one of the most frequently considered schemes for Biot's model is a three-field formulation based on piecewise linear elements for displacements, Raviart–Thomas–Nédélec elements for the fluid flux, and piecewise constants for the pressure, that is, the so-called $\mathbb{P}_1$–RT–$\mathbb{P}_0$ scheme. This finite element scheme, however, does not satisfy an inf-sup condition uniformly with respect to the physical parameters of the problem, and therefore, in [20] we proposed a stabilization of this popular element which gives rise to uniform error bounds, which is the discretization that we consider here.

More specifically, to discretize displacements we choose a piecewise linear continuous finite-element space, $\boldsymbol{V}_{h,1}$, enriched with edge/face (2D/3D) bubble functions, $\boldsymbol{V}_b$, that is $\boldsymbol{V}_h = \boldsymbol{V}_{h,1} \oplus \boldsymbol{V}_b$ (see [65, pp. 145–149]), for Darcy's velocity $\boldsymbol{W}_h$ is the lowest order Raviart–Thomas–Nédélec space (RT0), that is, $\boldsymbol{W}_h = \{\boldsymbol{w}_h \in \boldsymbol{W} \mid \boldsymbol{w}_h|_T = \boldsymbol{a} + \eta \boldsymbol{x},\ \boldsymbol{a} \in \mathbb{R}^d,\ \forall T \in \mathcal{T}_h\}$, and we use a piecewise constant space ($\mathbb{P}_0$) for Q_h in order to approximate the pressure field. Thus, any $\boldsymbol{u}_h \in \boldsymbol{V}_h$ can be written as $\boldsymbol{u}_h = \boldsymbol{u}_h^l + \boldsymbol{u}_h^b$, with $\boldsymbol{u}_h^l \in \boldsymbol{V}_{h,1}$ and $\boldsymbol{u}_h^b \in \boldsymbol{V}_b$, and we can rewrite system (37) as follows,

$$\mathcal{A} \begin{pmatrix} \boldsymbol{u}_h^b \\ \boldsymbol{u}_h^l \\ p_h \\ \boldsymbol{w}_h \end{pmatrix} = \boldsymbol{b}, \quad \text{with } \mathcal{A} = \begin{pmatrix} A_{bb} & A_{bl} & \alpha B_b^T & 0 \\ A_{bl}^T & A_{ll} & \alpha B_l^T & 0 \\ -\alpha B_b & -\alpha B_l & \frac{1}{M_b} M_p & -\tau B_{\boldsymbol{w}} \\ 0 & 0 & \tau B_{\boldsymbol{w}}^T & \tau M_{\boldsymbol{w}} \end{pmatrix}, \tag{38}$$

where $\boldsymbol{u}_b$, $\boldsymbol{u}_l$, p, and $\boldsymbol{w}$ are the unknown vectors for the bubble components of the displacement, the piecewise linear components of the displacement, the pressure, and the Darcy velocity, respectively. New blocks in the definition of matrix $\mathcal{A}$ correspond to the following bilinear forms:

$$\begin{aligned} &a(\boldsymbol{u}_h^b, \boldsymbol{v}_h^b) \to A_{bb}, \quad a(\boldsymbol{u}_h^l, \boldsymbol{v}_h^b) \to A_{bl}, \quad a(\boldsymbol{u}_h^l, \boldsymbol{v}_h^l) \to A_{ll}, \\ &-(\operatorname{div} \boldsymbol{u}_h^b, q_h) \to B_b, \quad -(\operatorname{div} \boldsymbol{u}_h^l, q_h) \to B_l, \end{aligned}$$

and are related to those in (37) by $A_{\boldsymbol{u}} = \begin{pmatrix} A_{bb} & A_{bl} \\ A_{lb} & A_{ll} \end{pmatrix}$ and $B_{\boldsymbol{u}} = \begin{pmatrix} B_b & B_l \end{pmatrix}$.

The well-posedness of the discretized system provides a convenient framework with which to construct block preconditioners, and in order to obtain parameter-robust preconditioners, such well-posedness property must hold independently to the discretization and physical parameters. In order to demonstrate such a uniform stability of the discrete system, we introduce the following weighted norm, for $\boldsymbol{x} = (\boldsymbol{u}, p, \boldsymbol{w})^T \in \boldsymbol{X} = \boldsymbol{V}_h \times Q_h \times \boldsymbol{W}_h$,

$$|||\boldsymbol{x}||| := \left[\|\boldsymbol{u}\|_{A_{\boldsymbol{u}}}^2 + c_p^{-1} \|p\|_{M_p}^2 + \tau \|\boldsymbol{w}\|_{M_{\boldsymbol{w}}}^2 + \tau^2 c_p \|B_{\boldsymbol{w}} \boldsymbol{w}\|_{M_p^{-1}}^2 \right]^{1/2}, \tag{39}$$

where $c_p := \left(\frac{\alpha^2}{\zeta^2} + \frac{1}{M_b} \right)^{-1}$ with $\zeta := \sqrt{\lambda + 2\mu/d}$ as before, and $d = 2$ or 3 is the dimension of the problem. Next, for $\boldsymbol{x} = (\boldsymbol{u}, p, \boldsymbol{w})$, $\boldsymbol{y} = (\boldsymbol{v}, q, \boldsymbol{r})$, we introduce the following composite bilinear form

$$\begin{aligned} \mathcal{L}(\boldsymbol{x}, \boldsymbol{y}) := {} & a(\boldsymbol{u}, \boldsymbol{v}) - (\alpha p, \operatorname{div} \boldsymbol{v}) + \tau (\boldsymbol{K}^{-1} \mu_f \boldsymbol{w}, \boldsymbol{r}) - \tau (p, \operatorname{div} \boldsymbol{r}) \\ & - \left(\frac{1}{M_b} p, q \right) - (\alpha \operatorname{div} \boldsymbol{u}, q) - \tau (\operatorname{div} \boldsymbol{w}, q). \end{aligned} \tag{40}$$

Then, in [20], it was shown that under certain conditions (referred to as Stokes–Biot stability [20, Def. 3.1]) on the space $\boldsymbol{X}$, the block matrix form $\mathcal{A}$ defined in (38) is well-posed with respect to the weighted norm (39).

Theorem 4 *If the triple $(\boldsymbol{V}_h, \boldsymbol{W}_h, Q_h)$ is Stokes–Biot stable, that is,*

- $a(\boldsymbol{u}, \boldsymbol{v}) \le C_V \|\boldsymbol{u}\|_1 \|\boldsymbol{v}\|_1$, *for all* $\boldsymbol{u}, \boldsymbol{v} \in \boldsymbol{V}_h$,
- $a(\boldsymbol{u}, \boldsymbol{v}) \ge \alpha_V \|\boldsymbol{u}\|_1^2$, *for all* $\boldsymbol{u} \in \boldsymbol{V}_h$,
- *The pair of spaces $(\boldsymbol{W}_h, Q_h)$ is Poisson stable, i.e., it satisfies stability and continuity conditions required by the mixed discretization of the Poisson equation,*
- *The pair of spaces $(\boldsymbol{V}_h, Q_h)$ is Stokes stable,*

then, it is fulfilled that $\mathcal{L}(\cdot,\cdot)$ is continuous with respect to $|||\cdot|||$, and the following inf-sup condition holds,

$$\inf_{\mathbf{0}\neq \boldsymbol{x}\in X}\sup_{\mathbf{0}\neq \boldsymbol{y}\in X}\frac{\mathcal{L}(\boldsymbol{x},\boldsymbol{y})}{|||\boldsymbol{x}|||\,|||\boldsymbol{y}|||}\geq \gamma, \tag{41}$$

where the constants involved are independent of mesh size h, time step size τ, and the physical parameters.

Proof The proof follows directly from Case I in the proof found in [21, Theorem 6], although the weighted norm used here is slightly different from the norm used in [21]. □

Next, we use the well-posedness property to develop block preconditioners for $\mathcal{A}$. Following the general framework previously introduced, we first consider block diagonal preconditioners (norm-equivalent preconditioners) and then we discuss block triangular (upper and lower) preconditioners following the framework developed for Field-of-Value (FOV) equivalent preconditioners. For both cases, the theoretical bounds on their performance remain independent of the discretization and physical parameters of the problem.

Norm-equivalent preconditioners

Since system (38) satisfies inf-sup condition (41), based on the framework proposed in Sect. 2.1, a natural choice for a norm-equivalent preconditioner is the Riesz operator with respect to the inner product corresponding to weighted norm (39), that is,

$$\mathcal{B}_D=\begin{pmatrix} A_{\boldsymbol{u}} & 0 & 0\\ 0 & \left(\frac{\alpha^2}{\zeta^2}+\frac{1}{M_b}\right)M_p & 0\\ 0 & 0 & \tau M_{\boldsymbol{w}}+\tau^2\left(\frac{\alpha^2}{\zeta^2}+\frac{1}{M_b}\right)^{-1}A_{\boldsymbol{w}}\end{pmatrix}^{-1}, \tag{42}$$

where $A_{\boldsymbol{w}}:=B_{\boldsymbol{w}}^T M_p^{-1}B_{\boldsymbol{w}}$.

In order to avoid the need of inverting exactly the diagonal blocks, we also propose the following inexact preconditioner,

$$\widehat{\mathcal{B}}_D=\begin{pmatrix} S_{\boldsymbol{u}} & 0 & 0\\ 0 & S_p & 0\\ 0 & 0 & S_{\boldsymbol{w}}\end{pmatrix}. \tag{43}$$

which is obtained by replacing the diagonal blocks in (42) by their spectrally-equivalent symmetric and positive definite approximations, $S_{\boldsymbol{u}}$, S_p and $S_{\boldsymbol{w}}$, satisfying that

$$c_{1,\boldsymbol{u}}(S_{\boldsymbol{u}}\boldsymbol{u},\boldsymbol{u})\leq(A_{\boldsymbol{u}}^{-1}\boldsymbol{u},\boldsymbol{u})\leq c_{2,\boldsymbol{u}}(S_{\boldsymbol{u}}\boldsymbol{u},\boldsymbol{u}), \tag{44}$$

$$c_{1,p}(S_p p,p)\leq\left(\left(\frac{\alpha^2}{\zeta^2}+\frac{1}{M_b}\right)^{-1}M_p^{-1}p,p\right)\leq c_{2,p}(S_p p,p), \tag{45}$$

$$c_{1,\boldsymbol{w}}(S_{\boldsymbol{w}}\boldsymbol{w},\boldsymbol{w})\leq\left(\left(\tau M_{\boldsymbol{w}}+\tau^2\left(\frac{\alpha^2}{\zeta^2}+\frac{1}{M_b}\right)^{-1}A_{\boldsymbol{w}}\right)^{-1}\boldsymbol{w},\boldsymbol{w}\right)\leq c_{2,\boldsymbol{w}}(S_{\boldsymbol{w}}\boldsymbol{w},\boldsymbol{w}), \tag{46}$$

where the involved constants $c_{1,\boldsymbol{u}}$, $c_{1,p}$, $c_{1,\boldsymbol{w}}$, $c_{2,\boldsymbol{u}}$, $c_{2,p}$, and $c_{2,\boldsymbol{w}}$ are independent of discretization and physical parameters.

In practice, naturally $S_{\boldsymbol{u}}$ can be defined by standard multigrid methods, and S_p is obtained by a diagonal scaling such that $S_p=\left(\frac{\alpha^2}{\zeta^2}+\frac{1}{M_b}\right)^{-1}M_p^{-1}$ since when using $\mathbb{P}_0$ elements

M_p results to be diagonal. The choice of $S_{\boldsymbol{w}}$, however, may require special attention since for large values of τ matrix $\tau M_{\boldsymbol{w}} + \tau^2 \left(\frac{\alpha^2}{\zeta^2} + \frac{1}{M_b}\right)^{-1} A_{\boldsymbol{w}}$ is numerically close to singular and then special preconditioners are needed. In particular, $S_{\boldsymbol{w}}$ can be defined by either an HX-preconditioner (Auxiliary Space Preconditioner) [53, 66] or multigrid with special block smoothers [52].

FOV-equivalent preconditioners

Following the FOV-equivalent framework previously introduced in Sect. 2.2, next, we consider more general preconditioners. In particular, block triangular preconditioners are designed for the linear system given in (38).

We first consider the block lower triangular preconditioner,

$$\mathcal{B}_L = \begin{pmatrix} A_{\boldsymbol{u}} & 0 & 0 \\ -\alpha B_{\boldsymbol{u}} & \left(\frac{\alpha^2}{\zeta^2} + \frac{1}{M_b}\right) M_p & 0 \\ 0 & \tau B_{\boldsymbol{w}}^T & \tau M_{\boldsymbol{w}} + \tau^2 \left(\frac{\alpha^2}{\zeta^2} + \frac{1}{M_b}\right)^{-1} A_{\boldsymbol{w}} \end{pmatrix}^{-1}, \tag{47}$$

for which we can prove the FOV-equivalence property in (8), that is,

Theorem 5 *Assuming a shape regular mesh and the discretization described above, there exist constants Σ and Υ, independent of discretization and physical parameters, such that, for any $\boldsymbol{x} = (\boldsymbol{u}, p, \boldsymbol{w})^T \neq \mathbf{0}$,*

$$\Sigma \leq \frac{(\mathcal{B}_L \mathcal{A}\boldsymbol{x}, \boldsymbol{x})_{(\mathcal{B}_D)^{-1}}}{(\boldsymbol{x}, \boldsymbol{x})_{(\mathcal{B}_D)^{-1}}}, \quad \frac{\|\mathcal{B}_L \mathcal{A}\boldsymbol{x}\|_{(\mathcal{B}_D)^{-1}}}{\|\boldsymbol{x}\|_{(\mathcal{B}_D)^{-1}}} \leq \Upsilon.$$

Analogously to the two-field formulation case, we also consider an inexact approach to the lower triangular preconditioner given as follows,

$$\widehat{\mathcal{B}}_L = \begin{pmatrix} S_{\boldsymbol{u}}^{-1} & 0 & 0 \\ -\alpha B_{\boldsymbol{u}} & S_p^{-1} & 0 \\ 0 & \tau B_{\boldsymbol{w}}^T & S_{\boldsymbol{w}}^{-1} \end{pmatrix}^{-1}, \tag{48}$$

where $S_{\boldsymbol{u}}$, S_p and $S_{\boldsymbol{w}}$, satisfy the spectral equivalence relations (44)–(46) and can be chosen in practice as we have specified in the previous section. Thus, $\mathcal{B}_L$ also satisfies the FOV-equivalence property, as stated in the following theorem.

Theorem 6 *If $\|I - S_{\boldsymbol{u}} A_{\boldsymbol{u}}\|_{A_{\boldsymbol{u}}} \leq \rho \leq 0.2228$, and $S_p = \left(\frac{\alpha^2}{\zeta^2} + \frac{1}{M_b}\right)^{-1} M_p^{-1}$, then there exists constants Σ and Υ, independent of discretization and physical parameters, such that, for any $\boldsymbol{x} = (\boldsymbol{u}, p, \boldsymbol{w})^T \neq \mathbf{0}$,*

$$\Sigma \leq \frac{\left(\widehat{\mathcal{B}}_L \mathcal{A}\boldsymbol{x}, \boldsymbol{x}\right)_{(\widehat{\mathcal{B}}_D)^{-1}}}{(\boldsymbol{x}, \boldsymbol{x})_{(\widehat{\mathcal{B}}_D)^{-1}}}, \quad \frac{\|\widehat{\mathcal{B}}_L \mathcal{A}\boldsymbol{x}\|_{(\widehat{\mathcal{B}}_D)^{-1}}}{\|\boldsymbol{x}\|_{(\widehat{\mathcal{B}}_D)^{-1}}} \leq \Upsilon.$$

The proofs of the above two theorems turn out to be a special case of some of the proofs included in [47], and thus are omitted here. With these results, we can use the theoretical framework introduced in Sect. 2.2 and then $\mathcal{B}_L$ and $\widehat{\mathcal{B}}_L$ result to be parameter-robust preconditioners for the GMRES method.

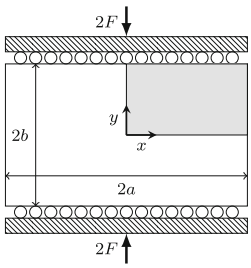

Fig. 2 2D physical and computational domain for Mandel's problem

Similar arguments can also be applied for the design of block upper triangular preconditioners, so that we can consider

$$\mathcal{B}_U = \begin{pmatrix} A_{\boldsymbol{u}} & \alpha B_{\boldsymbol{u}}^T & 0 \\ 0 & \left(\frac{\alpha^2}{\zeta^2} + \frac{1}{M_b}\right) M_p & -\tau B_{\boldsymbol{w}} \\ 0 & \upsilon 0 & \tau M_{\boldsymbol{w}} + \tau^2 \left(\frac{\alpha^2}{\zeta^2} + \frac{1}{M_b}\right)^{-1} A_{\boldsymbol{w}} \end{pmatrix}^{-1}, \tag{49}$$

and the corresponding inexact preconditioner,

$$\widehat{\mathcal{B}}_U = \begin{pmatrix} S_{\boldsymbol{u}}^{-1} & \alpha B_{\boldsymbol{u}}^T & 0 \\ 0 & S_p^{-1} & -\tau B_{\boldsymbol{w}} \\ 0 & 0 & S_{\boldsymbol{w}}^{-1} \end{pmatrix}^{-1}. \tag{50}$$

Analogous theorems to Theorems 5 and 6 can be stated, so that the FOV-equivalence property for $\mathcal{B}_U$ and $\widehat{\mathcal{B}}_U$ can be proved, giving rise to parameter robustness for the block upper triangular preconditioners.

Numerical experiment: Mandel's problem

We consider Mandel's problem in two-dimensions, which models an infinitely long saturated porous slab sandwiched between a top and bottom rigid frictionless plate. At time $t = 0$, each plate is loaded with a constant vertical force of magnitude $2F$ per unit length as shown in Fig. 2.

This problem is an important benchmarking tool as the analytical solution is known [67], and therefore, it has been widely used in the literature to test numerical methods for poroelastic problems. The analytical solution for pressure is given by

$$p(x, y, t) = 2p_0 \sum_{n=1}^{\infty} \frac{\sin \alpha_n}{\alpha_n - \sin \alpha_n \cos \alpha_n} \left(\cos \frac{\alpha_n x}{a} - \cos \alpha_n\right) \exp\left(\frac{-\alpha_n^2 ct}{a^2}\right), \tag{51}$$

where $p_0 = \frac{1}{3a} B(1 + \nu_u)F$, $B = 1$ is the Skempton's coefficient, $\nu_u = \frac{3\nu + B(1-2\nu)}{3 - B(1-2\nu)}$ is the undrained Poisson ratio, c is the consolidation coefficient given by $c = K(\lambda + 2\mu)$, and α_n are the positive roots to the nonlinear equation,

$$\tan \alpha_n = \frac{1 - \nu}{\nu_u - \nu} \alpha_n.$$

Due to symmetry of the problem we only need to solve in the top right quadrant, defined as $\Omega = (0, 1) \times (0, 1)$. We cover Ω with a uniform triangular grid by dividing an $N \times N$ uniform square grid into right triangles, where the mesh spacing is defined by $h = \frac{1}{N}$. For the material properties, $\mu_f = 1$, $\alpha = 1$, and $M_b = 10^6$, the Lamé coefficients are computed in terms of the Young's modulus, which is fixed to be $E = 10^4$, and the Poisson's ratio, ν. This

Table 3 Three-field stabilized $\mathbb{P}_1-\text{RT}-\mathbb{P}_0$ scheme: iteration counts for the block preconditioners with varying discretization parameters

	$\mathcal{B}_D$					$\mathcal{B}_L$					$\mathcal{B}_U$				
τ/h	$\frac{1}{8}$	$\frac{1}{16}$	$\frac{1}{32}$	$\frac{1}{64}$	$\frac{1}{128}$	$\frac{1}{8}$	$\frac{1}{16}$	$\frac{1}{32}$	$\frac{1}{64}$	$\frac{1}{128}$	$\frac{1}{8}$	$\frac{1}{16}$	$\frac{1}{32}$	$\frac{1}{64}$	$\frac{1}{128}$
0.1	39	40	40	40	38	19	19	18	17	17	19	19	19	18	17
0.01	26	34	39	39	38	15	18	19	18	17	14	17	18	18	17
0.001	23	23	28	34	37	11	12	15	17	18	10	11	14	17	17
0.0001	21	21	21	21	21	11	10	10	13	15	8	9	9	12	14
	$\widehat{\mathcal{B}}_D$					$\widehat{\mathcal{B}}_L$					$\widehat{\mathcal{B}}_U$				
τ/h	$\frac{1}{8}$	$\frac{1}{16}$	$\frac{1}{32}$	$\frac{1}{64}$	$\frac{1}{128}$	$\frac{1}{8}$	$\frac{1}{16}$	$\frac{1}{32}$	$\frac{1}{64}$	$\frac{1}{128}$	$\frac{1}{8}$	$\frac{1}{16}$	$\frac{1}{32}$	$\frac{1}{64}$	$\frac{1}{128}$
0.1	39	40	40	40	36	19	20	19	19	18	19	19	19	18	20
0.01	26	34	39	39	38	15	18	19	19	18	14	17	18	18	17
0.001	23	23	23	34	37	11	13	15	17	18	10	12	15	17	17
0.0001	21	22	21	23	29	11	11	11	13	15	9	9	10	12	15

latter, as well as the permeability tensor, $\boldsymbol{K}$, will be varied in order to show the robustness of the proposed preconditioners with respect to the physical parameters. In all test cases, we consider a diagonal permeability tensor $\boldsymbol{K} = K\boldsymbol{I}$, with constant K.

Next, we test the performance of the proposed block preconditioners, $\mathcal{B}_D$, $\mathcal{B}_L$, $\mathcal{B}_U$, $\widehat{\mathcal{B}}_D$, $\widehat{\mathcal{B}}_L$, and $\widehat{\mathcal{B}}_U$, with respect to discretization and physical parameters. For each test we use flexible GMRES to solve the linear system obtained from the bubble-enriched $\mathbb{P}_1-\text{RT0}-\mathbb{P}_0$ discretization. A stopping tolerance of 10^{-8} was used for the relative residual of the linear system, measured relative to the norm of the right hand side. The exact solves for the blocks in $\mathcal{B}_D$, $\mathcal{B}_L$, and $\mathcal{B}_U$ are done using the UMFPACK library [68–71]. For the inexact preconditioners, $S_{\boldsymbol{u}}$ is inverted using GMRES preconditioned with unsmoothed aggregation AMG in a V-cycle, solved to a relative residual tolerance of 10^{-3}, the $S_{\boldsymbol{w}}$ block is solved using an auxiliary space preconditioned GMRES to a relative residual tolerance of 10^{-3} [52, 53, 66], and the action of S_p is directly computed, since using a piecewise constant finite-element space for pressure results in a diagonal matrix for M_p.

First, we study the robustness of the preconditioners with respect to the discretization parameters. Thus, next test covers different values for the mesh size and the time step size, while the physical parameters are fixed as $\nu = 0.0$ and $K = 10^{-6}$. Then, in Table 3, we show the number of preconditioned GMRES iterations needed to solve the full bubble system up the required tolerance, by using the proposed exact and inexact block preconditioners and for different mesh sizes and time-step sizes. We can observe from the relatively consistent iteration counts the robustness of the preconditioners with respect to the discretization parameters. Since the block upper and lower triangular preconditioners contain more coupling information than the block diagonal preconditioners, as a result we see that they preform better than the block diagonal preconditioners. Finally, it is also important to notice that the performance impact of using the inexact block preconditioners is negligible versus using the exact block preconditioners, which implies that the inexact preconditioners could potentially be solved with less strict tolerance, resulting in more computational efficiency.

Next, we analyze the robustness of the proposed preconditioners with respect to the physical parameters. In order to do that, the mesh size is fixed to $h = \frac{1}{128}$ and the time-step size is

Table 4 Three-field stabilized $\mathbb{P}_1-\text{RT}-\mathbb{P}_0$ scheme: iteration counts for the block preconditioners with varying physical parameters K and ν

	$\nu = 0.0$ and varying K						$K = 10^{-6}$ and varying ν					
	1	10^{-2}	10^{-4}	10^{-6}	10^{-8}	10^{-10}	0.1	0.2	0.4	0.45	0.49	0.499
$\mathcal{B}_D$	23	25	35	38	29	19	45	52	39	36	28	20
$\mathcal{B}_L$	7	11	15	17	15	9	16	19	11	11	9	10
$\mathcal{B}_U$	13	16	17	16	15	7	20	22	16	14	11	16
$\widehat{\mathcal{B}}_D$	35	33	36	38	29	19	45	52	39	26	23	17
$\widehat{\mathcal{B}}_L$	14	15	16	18	15	10	17	20	14	12	11	12
$\widehat{\mathcal{B}}_U$	27	22	17	17	15	8	21	24	17	16	10	16

assumed to be $\tau = 0.01$, whereas the physical values of ν and K are varied. Then, in Table 4 we show the corresponding iteration counts for the block preconditioned GMRES.

On the left part of the table, we present the results obtained when the Poisson's ratio is fixed as $\nu = 0.0$ and the permeability varies from 1 to 10^{-10}, and on the right part of the table the permeability is fixed as $K = 10^{-6}$ whereas different values for the Poisson's ratio are considered, even approaching the incompressible material case ($\nu = 0.5$). Again, we observe robustness of the proposed preconditioners, this time with respect to the physical parameters. In addition, we can see that the use of the inexact preconditioners has minimal impact on their performance. Finally, notice that an interesting result is the better performance when the system is approaching the two considered limit cases, namely in the limit of impermeability ($K \to 0$) and in the limit of incompressibility ($\nu \to 0.5$).

Remark. Bubble eliminated system
A noteworthy result of [20] is that the degrees of freedom added to the faces to obtain the stabilized scheme can be eliminated resulting in a stable scheme with the same number of unknowns as in the initial $\mathbb{P}_1-\text{RT0}-\mathbb{P}_0$ discretization. In particular, one can replace the enrichment bubble block, A_{bb}, in (37) with a spectrally equivalent diagonal matrix, $D_{bb} := (d+1)\text{diag}(A_{bb})$, obtaining the following linear operator,

$$\mathcal{A}^D = \begin{pmatrix} D_{bb} & A_{bl} & \alpha B_b^T & 0 \\ A_{bl}^T & A_{ll} & \alpha B_l^T & 0 \\ -\alpha B_b & -\alpha B_l & \frac{1}{M_b} M_p & -\tau B_{\boldsymbol{w}} \\ 0 & 0 & \tau B_{\boldsymbol{w}}^T & \tau M_{\boldsymbol{w}} \end{pmatrix}, \tag{52}$$

where the stabilization term can be eliminated in a straightforward way by static condensation, yielding,

$$\mathcal{A}^E = \begin{pmatrix} A_{ll} - A_{bl}^T D_{bb}^{-1} A_{bl} & \alpha B_l^T - \alpha A_{bl}^T D_{bb}^{-1} B_b^T & 0 \\ -\alpha B_l + \alpha B_b D_{bb}^{-1} A_{bl} & \frac{1}{M_b} M_p + \alpha^2 B_b D_{bb}^{-1} B_b^T & -\tau B_{\boldsymbol{w}} \\ 0 & \tau B_{\boldsymbol{w}}^T & \tau M_{\boldsymbol{w}} \end{pmatrix}. \tag{53}$$

In such a way, an optimal stable discretization with the lowest possible number of degrees of freedom, equivalent to a discretization with $\mathbb{P}_1-\text{RT0}-\mathbb{P}_0$ elements, is obtained.

Due to the spectral equivalence between A_{bb} and D_{bb}, the formulation (52) is still well-posed (see [20]), and remains well-posed independently of the physical and discretization parameters. Since (37) is indefinite, the well-posedness of (53) does not simply follow directly, but it was proved in [47], where this well-posedness allowed the design of block preconditioners for the "bubble-eliminated system" given in (53).

3.2.2 Non conforming CR−RT−$\mathbb{P}_0$

Finally, we consider a stable finite element method for the three-field formulation of Biot's model that was proposed in [19] to avoid non-physical oscillations in the pressure field by using the lowest possible approximation order. This scheme considers a nonconforming finite element space for the displacements $\boldsymbol{u}$ and conforming finite element spaces for both the Darcy velocity $\boldsymbol{w}$ and the pressure p. More concretely, as in Sect. 3.2.1, $\boldsymbol{W}_h$ is the lowest order Raviart–Thomas–Nédélec space [72–74], and Q_h is the space of piecewise constant functions with respect to the triangulation $\mathcal{T}_h$, that is, $\mathbb{P}_0$. Regarding the displacements, $\boldsymbol{V}_h$ is chosen as the Crouzeix–Raviart finite element space [75], which consists of vector valued functions which are linear on every element $T \in \mathcal{T}_h$ and satisfy the following continuity conditions

$$\boldsymbol{V}_h = \left\{ \boldsymbol{v}_h \in \boldsymbol{L}^2(\Omega) \;\middle|\; \int_e [\![\boldsymbol{v}_h]\!]_e = 0, \quad \text{for all } e \in \mathcal{E}^o \right\},$$

where $[\![\boldsymbol{v}_h]\!]_e$ denotes the jump across an interior face $e \in \mathcal{E}^o$ for a given function $\boldsymbol{v}_h$.

Then $(\boldsymbol{u}_h^m, p_h^m, \boldsymbol{w}_h^m) \in \boldsymbol{V}_h \times Q_h \times \boldsymbol{W}_h$ must satisfy the discrete formulation in (34)–(36). However, if we simply take $a_h(\cdot,\cdot) = a(\cdot,\cdot)$, as done before, Korn's inequality may fail for the standard discretization by Crouzeix–Raviart elements without additional stabilization, and, therefore, $a_h(\cdot,\cdot)$ is not coercive. It is also possible that Korn's inequality hold, but the coercivity constant will approach infinity, blowing up, as the mesh size h approaches zero. For more details on nonconforming linear elements for elasticity problems and discrete Korn's inequality, we refer to [76, 77].

In order to fix such a problem, we can consider the following perturbation of the bilinear form which does satisfy the Korn's inequality and was proposed by Hansbo and Larson [78],

$$a_h(\boldsymbol{v}, \boldsymbol{w}) = a(\boldsymbol{v}, \boldsymbol{w}) + a_J(\boldsymbol{v}, \boldsymbol{w}), \quad \text{where} \quad a_J(\boldsymbol{v}, \boldsymbol{w}) = 2\mu\gamma_1 \sum_{e \in \mathcal{E}} h_e^{-1} \int_e [\![\boldsymbol{v}]\!]_e [\![\boldsymbol{w}]\!]_e,$$

where $\mathcal{E}$ denotes the set of faces (interfaces) in the triangulation $\mathcal{T}_h$, and constant $\gamma_1 > 0$ is a fixed real number away from 0 (i.e. $\gamma_1 = \frac{1}{2}$ is an acceptable choice). As shown in Hansbo and Larson [78] the bilinear form $a_h(\cdot,\cdot)$ is positive definite and the corresponding error is of optimal (first) order in the corresponding energy norm. Moreover, the resulting method is *locking free* and therefore we use such $a_h(\cdot,\cdot)$ in our nonconforming scheme (see more details in [19]. Regarding the bilinear form corresponding to the term $(\boldsymbol{K}^{-1}\mu_f \boldsymbol{w}_h^m, \boldsymbol{r}_h)$ in (36), the standard choice is just taking the usual $L^2(\Omega)$ inner product, leading to a mass matrix in the Raviart–Thomas–Nédélec element. Here, however, we use mass lumping in the Raviart–Thomas space, since it actually gives an oscillation-free approximation while maintains optimal error estimates (see [19]). Notice that such lumped mass approximation results in a block diagonal matrix and, therefore, it allows to eliminate the Darcy velocity and reduce the three-field formulation to a two-field formulation involving only displacement and pressure, reducing the size of the linear system to solve at each time step and consequently saving computational cost.

Considering all these modifications with respect to the three-field discrete formulation introduced in the previous sections, we can define the corresponding composite bilinear form $\mathcal{L}(\boldsymbol{x}, \boldsymbol{y})$, as done in (40), and prove the well-posedness of the linear system $\mathcal{A}\boldsymbol{x} = \mathbf{b}$, with $\boldsymbol{x} = (\boldsymbol{u}, p, \boldsymbol{w})^T$ and $\mathcal{A} = \begin{pmatrix} A_{\boldsymbol{u}} & \alpha B_{\boldsymbol{u}}^T & 0 \\ -\alpha B_{\boldsymbol{u}} & 0 & -\tau B_{\boldsymbol{w}} \\ 0 & \tau B_{\boldsymbol{w}}^T & \tau I_{\boldsymbol{w}} \end{pmatrix}$, with respect to the weighted norm introduced in (39). Notice that we denote as $I_{\boldsymbol{w}}$ to the lumped mass matrix for Darcy's velocity, and that the first term in the flow equation is neglected by assuming that the fluid is incompressible, as we did in the two-field formulation section, so that we consider this challenging case also in the three-field formulation framework.

Theorem 7 *If the triple $(\boldsymbol{V}_h, \boldsymbol{W}_h, Q_h)$ is Stokes–Biot stable, then, it is fulfilled that $\mathcal{L}(\cdot, \cdot)$ is continuous with respect to $|||\cdot|||$, and the following inf-sup condition holds,*

$$\inf_{\mathbf{0}\neq\boldsymbol{x}\in X} \sup_{\mathbf{0}\neq\boldsymbol{y}\in X} \frac{\mathcal{L}(\boldsymbol{x}, \boldsymbol{y})}{|||\boldsymbol{x}||| \, |||\boldsymbol{y}|||} \geq \gamma, \tag{54}$$

where the constants involved are independent of mesh size h, time step size τ, and the physical parameters.

Proof The proof is as the well-posedness proof in [19], but considering the weighted norm (39). We do not include the proof here since it uses the same techniques than those applied in the previous proofs included in this work. □

Norm-equivalent preconditioners

After proving the well-posedness of the system, we can consider again as norm-equivalent preconditioner the Riesz operator with respect to the inner product associated with the weighted norm introduced in (39), that is,

$$\mathcal{B}_D = \begin{pmatrix} A_{\boldsymbol{u}} & 0 & 0 \\ 0 & \frac{\alpha^2}{\zeta^2} M_p & 0 \\ 0 & 0 & \tau I_{\boldsymbol{w}} + \tau^2 \frac{\zeta^2}{\alpha^2} A_{\boldsymbol{w}} \end{pmatrix}^{-1}. \tag{55}$$

This results in a parameter-robust block diagonal preconditioner for the solution of the considered Biot's three-field formulation.

By considering spectrally-equivalent SPD approximations of the diagonal blocks, we can construct the following inexact block diagonal preconditioner,

$$\widehat{\mathcal{B}}_D = \begin{pmatrix} S_{\boldsymbol{u}} & 0 & 0 \\ 0 & S_p & 0 \\ 0 & 0 & S_{\boldsymbol{w}} \end{pmatrix}, \tag{56}$$

where $S_{\boldsymbol{u}}$, S_p and $S_{\boldsymbol{w}}$ satisfy that

$$c_{1,\boldsymbol{u}}(S_{\boldsymbol{u}}\boldsymbol{u}, \boldsymbol{u}) \leq (A_{\boldsymbol{u}}^{-1}\boldsymbol{u}, \boldsymbol{u}) \leq c_{2,\boldsymbol{u}}(S_{\boldsymbol{u}}\boldsymbol{u}, \boldsymbol{u}), \tag{57}$$

$$c_{1,p}(S_p p, p) \leq \left(\frac{\zeta^2}{\alpha^2} M_p^{-1} p, p\right) \leq c_{2,p}(S_p p, p), \tag{58}$$

$$c_{1,\boldsymbol{w}}(S_{\boldsymbol{w}}\boldsymbol{w}, \boldsymbol{w}) \leq \left(\left(\tau I_{\boldsymbol{w}} + \tau^2 \frac{\zeta^2}{\alpha^2} A_{\boldsymbol{w}}\right)^{-1} \boldsymbol{w}, \boldsymbol{w}\right) \leq c_{2,\boldsymbol{w}}(S_{\boldsymbol{w}}\boldsymbol{w}, \boldsymbol{w}), \tag{59}$$

where the involved constants are independent of the discretization and physical parameters. As previously commented, again, $S_{\boldsymbol{u}}$ can be defined by multigrid methods, S_p is applied as

a Jacobi iteration since the original block results to be diagonal, and $S_{\boldsymbol{w}}$ can be defined by an auxiliary space method as the HX-preconditioner.

FOV-equivalent preconditioners
Next, we consider block triangular preconditioners, arising from the FOV-equivalent framework introduced in Sect. 2.2. In particular, the following block lower triangular preconditioner can be defined,

$$\mathcal{B}_L = \begin{pmatrix} A_{\boldsymbol{u}} & 0 & 0 \\ -\alpha B_{\boldsymbol{u}} & \frac{\alpha^2}{\lambda + \frac{2\mu}{d}} M_p & 0 \\ 0 & \tau B_{\boldsymbol{w}}^T & \tau I_{\boldsymbol{w}} + \frac{\tau^2}{\alpha^2}\left(\lambda + \frac{2\mu}{d}\right) A_{\boldsymbol{w}} \end{pmatrix}^{-1}, \tag{60}$$

as well as its inexact counterpart given by

$$\widehat{\mathcal{B}}_L = \begin{pmatrix} S_{\boldsymbol{u}}^{-1} & 0 & 0 \\ -\alpha B_{\boldsymbol{u}} & S_p^{-1} & 0 \\ 0 & \tau B_{\boldsymbol{w}}^T & S_{\boldsymbol{w}}^{-1}. \end{pmatrix}^{-1}, \tag{61}$$

where $S_{\boldsymbol{u}}$, S_p and $S_{\boldsymbol{w}}$ satisfy the spectral equivalence relations (57)–(59). These operators $\mathcal{B}_L$ and $\widehat{\mathcal{B}}_L$ satisfy that they are FOV-equivalent with $\mathcal{A}$, since we can prove analogous theorems to Theorems 5 and 6, and therefore they result in parameter-robust preconditioners for the GMRES method.

Analogously, we can also consider uniform right preconditioners given by the following block upper triangular operators,

$$\mathcal{B}_U = \begin{pmatrix} A_{\boldsymbol{u}} & \alpha B_{\boldsymbol{u}}^T & 0 \\ 0 & \frac{\alpha^2}{\lambda + \frac{2\mu}{d}} M_p & -\tau B_{\boldsymbol{w}} \\ 0 & 0 & \tau I_{\boldsymbol{w}} + \frac{\tau^2}{\alpha^2}\left(\lambda + \frac{2\mu}{d}\right) A_{\boldsymbol{w}} \end{pmatrix}^{-1}, \quad \widehat{\mathcal{B}}_U = \begin{pmatrix} S_{\boldsymbol{u}}^{-1} & \alpha B_{\boldsymbol{u}}^T & 0 \\ 0 & S_p^{-1} & -\tau B_{\boldsymbol{w}} \\ 0 & 0 & S_{\boldsymbol{w}}^{-1} \end{pmatrix}^{-1}. \tag{62}$$

Numerical experiment: poroelastic problem on a square domain with a uniform load
We consider a Terzaghi's type problem which models a column of poroelastic material $\Omega = (0, 1) \times (0, 1)$ which drains on the north (top) edge of the boundary, where also a uniform unit load is applied, that is,

$$p = 0, \quad \boldsymbol{\sigma} \cdot \mathbf{n} = (0, -1)^t, \text{ on } \Gamma_1 = [0, 1] \times 1.$$

The medium is assumed to be rigid and impermeable on the rest of the boundary, namely, the rest of the boundary conditions are:

$$\nabla p \cdot \mathbf{n} = 0, \quad \mathbf{u} = \mathbf{0}, \text{ on } \Gamma_2 = \partial\Omega \setminus \Gamma_1.$$

For clarity, the computational domain together with the prescribed boundary conditions are shown in Fig. 3.

Next, we test the performance of the proposed exact, $\mathcal{B}_D$, $\mathcal{B}_L$ and $\mathcal{B}_U$, and inexact, $\widehat{\mathcal{B}}_D$, $\widehat{\mathcal{B}}_L$ and $\widehat{\mathcal{B}}_U$, preconditioners with respect to different values of both the discretization and physical parameters. In order to do that, we consider the preconditioned flexible GMRES with a relative residual stopping criteria of 10^{-6}. Regarding the material properties, in this numerical experiment, we fix the Young's modulus $E = 3 \times 10^4$ N/m^2, and we will consider a diagonal permeability tensor $\boldsymbol{K} = K\boldsymbol{I}$, with K constant.

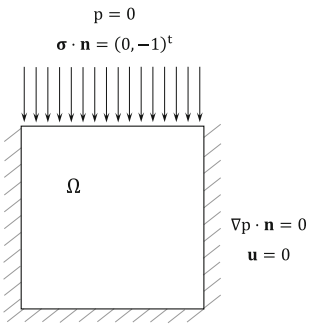

Fig. 3 Computational domain and boundary conditions corresponding to the poroelastic test problem on a square domain with a uniform load

Table 5 Three-field CR−RT−$\mathbb{P}_0$ scheme: Iteration counts for the block preconditioners for different values of the discretization parameters

	$\mathcal{B}_D$				$\mathcal{B}_L$				$\mathcal{B}_U$			
τ/h	$\frac{1}{8}$	$\frac{1}{16}$	$\frac{1}{32}$	$\frac{1}{64}$	$\frac{1}{8}$	$\frac{1}{16}$	$\frac{1}{32}$	$\frac{1}{64}$	$\frac{1}{8}$	$\frac{1}{16}$	$\frac{1}{32}$	$\frac{1}{64}$
0.1	42	46	48	52	22	23	24	25	23	24	26	27
0.01	41	43	47	47	22	22	23	25	20	21	23	24
0.001	41	43	43	47	22	22	23	24	18	18	21	22
0.0001	41	43	43	46	22	22	23	24	18	18	19	19
	$\widehat{\mathcal{B}}_D$				$\widehat{\mathcal{B}}_L$				$\widehat{\mathcal{B}}_U$			
τ/h	$\frac{1}{8}$	$\frac{1}{16}$	$\frac{1}{32}$	$\frac{1}{64}$	$\frac{1}{8}$	$\frac{1}{16}$	$\frac{1}{32}$	$\frac{1}{64}$	$\frac{1}{8}$	$\frac{1}{16}$	$\frac{1}{32}$	$\frac{1}{64}$
0.1	42	48	54	57	24	26	26	31	26	30	29	32
0.01	42	44	49	50	24	25	27	28	24	26	26	28
0.001	42	44	49	49	24	25	27	28	25	24	24	26
0.0001	42	46	49	50	24	25	27	28	25	29	30	30

We start by testing the robustness of the proposed preconditioners with respect to the discretization parameters. With this purpose, we fix the values of the permeability as $K = 10^{-6}$ and the Poisson's ratio as $\nu = 0.2$, and vary the spatial discretization parameter h from $1/8$ to $1/64$ and the time step size τ from 0.1 to 0.0001. For these values, in Table 5, we show the number of preconditioned GMRES iterations that are necessary to reduce the residual under the prescribed tolerance. From the iteration counts shown in the table, we can observe a robust behavior or the proposed preconditioners with respect to the discretization parameters. Also, we can derive similar conclusions to those mentioned in the numerical examples for the other considered numerical schemes, as for example, the good performance provided by the inexact counterparts of the proposed block preconditioners.

Finally, we want to show the robustness of the proposed preconditioned GMRES method with respect to the material parameters. With this aim, in Table 6, we provide iteration counts for the proposed block preconditioners for varying physical parameters. In particular, on the left part of Table 6, we assume a fixed value of the Poisson's ratio $\nu = 0.2$ and we choose the permeability K ranging from 1 to 10^{-10}, whereas on the right part of such a table, we fix the value of the permeability as $K = 10^{-6}$ and vary the value of ν from 0.1 to 0.499, approaching the incompressible material case. In both cases, we observe again a robust behavior of the proposed preconditioners.

Table 6 Three-field CR−RT−$\mathbb{P}_0$ scheme: iteration counts for the block preconditioners with varying physical parameters K and ν

	$\nu = 0.2$ and varying K						$K = 10^{-6}$ and varying ν					
	1	10^{-2}	10^{-4}	10^{-6}	10^{-8}	10^{-10}	0.1	0.2	0.4	0.45	0.49	0.499
$\mathcal{B}_D$	80	61	47	47	47	47	51	47	30	24	17	13
$\mathcal{B}_L$	54	41	23	23	23	23	26	23	15	12	9	7
$\mathcal{B}_U$	52	41	23	23	23	23	26	23	16	13	9	6
$\widehat{\mathcal{B}}_D$	98	63	49	49	49	49	53	49	35	29	24	21
$\widehat{\mathcal{B}}_L$	76	45	27	27	27	27	30	27	19	16	14	13
$\widehat{\mathcal{B}}_U$	68	44	30	30	30	30	33	30	22	17	18	20

4 Conclusions

In this work, we have presented an overview about the design of parameter-robust preconditioners for poromechanics problems. In particular we have considered different conforming and non-conforming discretizations proposed by the authors for the two- and three-field formulations of the Biot's model and we have proposed block diagonal and triangular preconditioners with a uniform performance with respect to discretization and physical parameters. We have explained how the stability and well-posedness of the discrete problem provides a foundation for designing such robust preconditioners which yield uniform convergence rates for Krylov subspace methods. We present theoretical results confirming the robustness of the proposed preconditioners with respect to mesh size, time step, and the physical parameters of the model, and finally we demonstrate this behavior with numerical experiments in which we consider well-known benchmark problems that are used in the literature for testing numerical methods for poroelastic problems.

Acknowledgements The work of Carmen Rodrigo is supported in part by the Spanish project PGC2018-099536-A-I00 (MCIU/AEI/FEDER, UE). Francisco J. Gaspar has received funding from the Spanish project PID2019-105574GB-I00 (MCIU/AEI/FEDER, UE). Carmen Rodrigo and Francisco J. Gaspar acknowledge support from the Diputación General de Aragón, Spain (Grupo de referencia APEDIF, ref. E24_17R). The work of Adler, Hu and Ohm is partially supported by the National Science Foundation (NSF) under Grant DMS-2208267. The research of Zikatanov is supported in part by the U. S.-Norway Fulbright Foundation and the U. S. National Science Foundation Grant DMS-2208249.

Funding Open Access funding provided thanks to the CRUE-CSIC agreement with Springer Nature.

Data availability Not applicable.

Declarations

Conflict of interest The authors declare that they have no conflict of interest.

References

1. Terzaghi, K.: Theoretical Soil Mechanics. Wiley, New York (1943). https://doi.org/10.1002/9780470172766
2. Biot, M.A.: General theory of three-dimensional consolidation. J. Appl. Phys. **12**(2), 155–164 (1941). https://doi.org/10.1063/1.1712886
3. Biot, M.A.: Theory of elasticity and consolidation for a porous anisotropic solid. J. Appl. Phys. **26**(2), 182–185 (1955). https://doi.org/10.1063/1.1721956
4. Lee, J.J., Mardal, K.-A., Winther, R.: Parameter-robust discretization and preconditioning of Biot's consolidation model. SIAM J. Sci. Comput. **39**(1), 1–24 (2017). https://doi.org/10.1137/15M1029473
5. Wang, H.F.: Theory of Linear Poroelasticity with Applications to Geomechanics and Hydrogeology. Princeton University Press, Princeton (2001). https://doi.org/10.1515/9781400885688
6. Ben-Hatira, F., Saidane, K., Mrabet, A.: A finite element modeling of the human lumbar unit including the spinal cord. J. Biomed. Sci. Eng. **5**, 146–152 (2012). https://doi.org/10.4236/jbise.2012.53019
7. Smith, J.H., Humphrey, J.A.: Interstitial transport and transvascular fluid exchange during infusion into brain and tumor tissue. Microvasc. Res. **73**(1), 58–73 (2007). https://doi.org/10.1016/j.mvr.2006.07.001
8. Støverud, K.H., Alnæs, M., Langtangen, H.P., Haughton, V., Mardal, K.-A.: Poro-elastic modeling of syringomyelia—a systematic study of the effects of pia mater, central canal, median fissure, white and gray matter on pressure wave propagation and fluid movement within the cervical spinal cord. Comput. Methods Biomech. Biomed. Eng. **19**(6), 686–698 (2016). https://doi.org/10.1080/10255842.2015.1058927
9. Axelsson, O., Blaheta, R., Byczanski, P.: Stable discretization of poroelasticity problems and efficient preconditioners for arising saddle point type matrices. Comput. Visual Sci. **15**, 191–207 (2012). https://doi.org/10.1007/s00791-013-0209-0
10. Gaspar, F.J., Lisbona, F.J., Vabishchevich, P.N.: A finite difference analysis of Biot's consolidation model. Appl. Numer. Math. **44**(4), 487–506 (2003). https://doi.org/10.1016/S0168-9274(02)00190-3
11. Gaspar, F.J., Lisbona, F.J., Vabishchevich, P.N.: Staggered grid discretizations for the quasi-static Biot's consolidation problem. Appl. Numer. Math. **56**(6), 888–898 (2006). https://doi.org/10.1016/j.apnum.2005.07.002
12. Nordbotten, J.M.: Stable cell-centered finite volume discretization for Biot equations. SIAM J. Numer. Anal. **54**(2), 942–968 (2016). https://doi.org/10.1137/15M1014280
13. Murad, M.A., Loula, A.F.D.: Improved accuracy in finite element analysis of Biot's consolidation problem. Comput. Methods Appl. Mech. Eng. **95**(3), 359–382 (1992). https://doi.org/10.1016/0045-7825(92)90193-N
14. Murad, M.A., Loula, A.F.D.: On stability and convergence of finite element approximations of Biot's consolidation problem. Int. J. Numer. Methods Eng. **37**(4), 645–667 (1994). https://doi.org/10.1002/nme.1620370407
15. Murad, M.A., Thomée, V., Loula, A.F.D.: Asymptotic behavior of semidiscrete finite-element approximations of Biot's consolidation problem. SIAM J. Numer. Anal. **33**(3), 1065–1083 (1996). https://doi.org/10.1137/0733052
16. Aguilar, G., Gaspar, F., Lisbona, F., Rodrigo, C.: Numerical stabilization of Biot's consolidation model by a perturbation on the flow equation. Int. J. Numer. Methods Eng. **75**(11), 1282–1300 (2008). https://doi.org/10.1002/nme.2295
17. Rodrigo, C., Gaspar, F., Hu, X., Zikatanov, L.: Stability and monotonicity for some discretizations of the Biot's consolidation model. Comput. Methods Appl. Mech. Eng. **298**, 183–204 (2016). https://doi.org/10.1016/j.cma.2015.09.019
18. Pé de la Riva, A., Gaspar, F., Rodrigo, C., Hu, X., Zikatanov, L.: Oscillation-free numerical schemes for the Biot's model with automatic stabilization. Submitted (2023)
19. Hu, X., Rodrigo, C., Gaspar, F.J., Zikatanov, L.T.: A nonconforming finite element method for the Biot's consolidation model in poroelasticity. J. Comput. Appl. Math. **310**, 143–154 (2017). https://doi.org/10.1016/j.cam.2016.06.003
20. Rodrigo, C., Hu, X., Ohm, P., Adler, J.H., Gaspar, F.J., Zikatanov, L.T.: New stabilized discretizations for poroelasticity and the Stokes' equations. Comput. Methods Appl. Mech. Eng. **341**, 467–484 (2018). https://doi.org/10.1016/j.cma.2018.07.003
21. Hong, Q., Kraus, J.: Parameter-robust stability of classical three-field formulation of Biot's consolidation model. Electron. Tran. Numer. Anal. **48**, 202–226 (2018). https://doi.org/10.1553/etna_vol48s202
22. Oyarzúa, R., Ruiz-Baier, R.: Locking-free finite element methods for poroelasticity. SIAM J. Numer. Anal. **54**(5), 2951–2973 (2016). https://doi.org/10.1137/15M1050082
23. Lee, J.J.: Robust error analysis of coupled mixed methods for Biot's consolidation model. J. Sci. Comput. **69**(2), 610–632 (2016). https://doi.org/10.1007/s10915-016-0210-0

24. Boon, W.M., Kuchta, M., Mardal, K.-A., Ruiz-Baier, R.: Robust preconditioners for perturbed saddle-point problems and conservative discretizations of biot's equations utilizing total pressure. SIAM J. Sci. Comput. **43**(4), 961–983 (2021). https://doi.org/10.1137/20M1379708
25. Kim, J., Tchelepi, H.A.A., Juanes, R.: Stability, accuracy, and efficiency of sequential methods for coupled flow and geomechanics. SPE J. **16**(02), 249–262 (2011). https://doi.org/10.2118/119084-PA
26. Kim, J.: Sequential methods for coupled geomechanics and multiphase flow. PhD thesis, Stanford University (2010)
27. Mikelić, A., Wheeler, M.F.: Convergence of iterative coupling for coupled flow and geomechanics. Comput. Geosci. **17**(3), 455–461 (2013). https://doi.org/10.1007/s10596-012-9318-y
28. Both, J.W., Borregales, M., Nordbotten, J.M., Kumar, K., Radu, F.A.: Robust fixed stress splitting for Biot's equations in heterogeneous media. Appl. Math. Lett. **68**, 101–108 (2017). https://doi.org/10.1016/j.aml.2016.12.019
29. Almani, T., Kumar, K., Dogru, A., Singh, G., Wheeler, M.F.: Convergence analysis of multirate fixed-stress split iterative schemes for coupling flow with geomechanics. Comput. Methods Appl. Mech. Eng. **311**, 180–207 (2016). https://doi.org/10.1016/j.cma.2016.07.036
30. Bause, M., Radu, F.A., Köcher, U.: Space-time finite element approximation of the Biot poroelasticity system with iterative coupling. Comput. Methods Appl. Mech. Eng. **320**, 745–768 (2017). https://doi.org/10.1016/j.cma.2017.03.017
31. Borregales, M., Kumar, K., Radu, F.A., Rodrigo, C., Gaspar, F.J.: A partially parallel-in-time fixed-stress splitting method for Biot's consolidation model. Comput. Math. Appl. **77**(6), 1466–1478 (2019). https://doi.org/10.1016/j.camwa.2018.09.005. (**7th International Conference on Advanced Computational Methods in Engineering (ACOMEN 2017)**)
32. Castelletto, N., White, J.A., Tchelepi, H.A.: Accuracy and convergence properties of the fixed-stress iterative solution of two-way coupled poromechanics. Int. J. Numer. Anal. Meth. Geomech. **39**(14), 1593–1618 (2015). https://doi.org/10.1002/nag.2400
33. White, J.A., Castelletto, N., Tchelepi, H.A.: Block-partitioned solvers for coupled poromechanics: a unified framework. Comput. Methods Appl. Mech. Eng. **303**, 55–74 (2016). https://doi.org/10.1016/j.cma.2016.01.008
34. Gaspar, F.J., Gracia, J.L., Lisbona, F.J., Oosterlee, C.W.: Distributive smoothers in multigrid for problems with dominating grad-div operators. Numer. Linear Algebra Appl. **15**(8), 661–683 (2008). https://doi.org/10.1002/nla.587
35. Gaspar, F.J., Lisbona, F.J., Oosterlee, C.W., Wienands, R.: A systematic comparison of coupled and distributive smoothing in multigrid for the poroelasticity system. Numer. Linear Algebra Appl. **11**(2–3), 93–113 (2004). https://doi.org/10.1002/nla.372
36. Luo, P., Rodrigo, C., Gaspar, F.J., Oosterlee, C.W.: On an Uzawa smoother in multigrid for poroelasticity equations. Numer. Linear Algebra Appl. **24**(1), 2074 (2017). https://doi.org/10.1002/nla.2074.e2074nla.2074
37. Gaspar, F.J., Rodrigo, C.: On the fixed-stress split scheme as smoother in multigrid methods for coupling flow and geomechanics. Comput. Methods Appl. Mech. Eng. **326**, 526–540 (2017). https://doi.org/10.1016/j.cma.2017.08.025
38. Adler, J.H., He, Y., Hu, X., MacLachlan, S., Ohm, P.: Monolithic multigrid for a reduced-quadrature discretization of poroelasticity. SIAM J. Sci. Comput. **20**, 54–81 (2022). https://doi.org/10.1137/21M1429072
39. Phoon, K.K., Toh, K.C., Chan, S.H., Lee, F.H.: An efficient diagonal preconditioner for finite element solution of Biot's consolidation equations. Int. J. Numer. Methods Eng. **55**(4), 377–400 (2002). https://doi.org/10.1002/nme.500
40. Bergamaschi, L., Ferronato, M., Gambolati, G.: Novel preconditioners for the iterative solution to FE-discretized coupled consolidation equations. Comput. Methods Appl. Mech. Eng. **196**(25), 2647–2656 (2007). https://doi.org/10.1016/j.cma.2007.01.013
41. Ferronato, M., Bergamaschi, L., Gambolati, G.: Performance and robustness of block constraint preconditioners in finite element coupled consolidation problems. Int. J. Numer. Methods Eng. **81**(3), 381–402 (2010). https://doi.org/10.1002/nme.2702
42. Haga, J.B., Osnes, H., Langtangen, H.P.: Efficient block preconditioners for the coupled equations of pressure and deformation in highly discontinuous media. Int. J. Numer. Anal. Methods Geomech. **35**(13), 1466–1482 (2011). https://doi.org/10.1002/nag.973
43. Castelletto, N., White, J.A., Ferronato, M.: Scalable algorithms for three-field mixed finite element coupled poromechanics. J. Comput. Phys. **327**, 894–918 (2016). https://doi.org/10.1016/j.jcp.2016.09.063
44. Bærland, T., Lee, J.J., Mardal, K.-A., Winther, R.: Weakly imposed symmetry and robust preconditioners for Biot's consolidation model. Comput. Methods Appl. Math. **17**(3), 377–396 (2017). https://doi.org/10.1515/cmam-2017-0016

45. Adler, J.H., Gaspar, F.J., Hu, X., Rodrigo, C., Zikatanov, L.T.: Robust block preconditioners for Biot's model. In: Bjørstad, P.E., Brenner, S.C., Halpern, L., Kim, H.H., Kornhuber, R., Rahman, T., Widlund, O.B. (eds.) Domain Decomposition Methods in Science and Engineering XXIV, pp. 3–16. Springer, Cham (2018). https://doi.org/10.1007/978-3-319-93873-8_1
46. Hong, Q., Kraus, J., Lymbery, M., Philo, F.: Conservative discretizations and parameter-robust preconditioners for Biot and multiple-network flux-based poroelasticity models. Numer. Linear Algebra Appl. **26**(4), 2242 (2019). https://doi.org/10.1002/nla.2242
47. Adler, J.H., Gaspar, F.J., Hu, X., Ohm, P., Rodrigo, C., Zikatanov, L.T.: Robust preconditioners for a new stabilized discretization of the poroelastic equations. SIAM J. Sci. Comput. **42**(3), 761–791 (2020). https://doi.org/10.1137/19M1261250
48. Chen, S., Hong, Q., Xu, J., Yang, K.: Robust block preconditioners for poroelasticity. Comput. Methods Appl. Mech. Eng. **369**, 113229 (2020). https://doi.org/10.1016/j.cma.2020.113229
49. Elman, H., Howle, V.E., Shadid, J., Shuttleworth, R., Tuminaro, R.: Block preconditioners based on approximate commutators. SIAM J. Sci. Comput. **27**(5), 1651–1668 (2006). https://doi.org/10.1137/040608817
50. Elman, H., Howle, V.E., Shadid, J., Shuttleworth, R., Tuminaro, R.: A taxonomy and comparison of parallel block multi-level preconditioners for the incompressible Navier–Stokes equations. J. Comput. Phys. **227**(3), 1790–1808 (2008). https://doi.org/10.1016/j.jcp.2007.09.026
51. Brandt, A., McCormick, S.F., Ruge, J.W.: Algebraic multigrid (AMG) for sparse matrix equations. In: Evans, D.J. (ed.) Sparsity and Its Applications. Cambridge University Press, Cambridge (1984)
52. Arnold, D.N., Falk, R.S., Winther, R.: Multigrid in H (div) and H (curl). Numer. Math. **85**(2), 197–217 (2000). https://doi.org/10.1007/PL00005386
53. Hiptmair, R., Xu, J.: Nodal auxiliary space preconditioning in H(curl) and H(div) spaces. SIAM J. Numer. Anal. **45**(6), 2483–2509 (2007). https://doi.org/10.1137/060660588
54. Loghin, D., Wathen, A.J.: Analysis of preconditioners for saddle-point problems. SIAM J. Sci. Comput. **25**(6), 2029–2049 (2004). https://doi.org/10.1137/S1064827502418203
55. Mardal, K.-A., Winther, R.: Preconditioning discretizations of systems of partial differential equations. Numer. Linear Algebra Appl. **18**(1), 1–40 (2011). https://doi.org/10.1002/nla.716
56. Klawonn, A., Starke, G.: Block triangular preconditioners for nonsymmetric saddle point problems: field-of-values analysis. Numer. Math. **81**(4), 577–594 (1999). https://doi.org/10.1007/s002110050405
57. Starke, G.: Field-Of-Values analysis of preconditioned iterative methods for nonsymmetric elliptic problems. Numer. Math. **78**, 103–117 (1997). https://doi.org/10.1007/s002110050306
58. Hu, X., Adler, J.H., Zikatanov, L.T.: HAZmath: a simple finite element, graph, and solver library. https://hazmathteam.github.io/hazmath/
59. Greenbaum, A.: Iterative Methods for Solving Linear Systems. Society for Industrial and Applied Mathematics, Philadelphia (1997). https://doi.org/10.1137/1.9781611970937
60. Elman, H.C.: Iterative methods for large, sparse, nonsymmetric systems of linear equations. PhD thesis, Yale University New Haven, Conn (1982)
61. Eisenstat, S.C., Elman, H.C., Schultz, M.H.: Variational iterative methods for nonsymmetric systems of linear equations. SIAM J. Numer. Anal. **20**(2), 345–357 (1983). https://doi.org/10.1137/0720023
62. Arnold, D.N., Brezzi, F., Fortin, M.: A stable finite element for the Stokes equations. Calcolo **21**(4), 337–344 (1985). https://doi.org/10.1007/BF02576171
63. Stenberg, R.: A technique for analysing finite element methods for viscous incompressible flow. Int. J. Numer. Methods Fluids **11**(6), 935–948 (1990). https://doi.org/10.1002/fld.1650110615. (**The Seventh International Conference on Finite Elements in Flow Problems (Huntsville, AL, 1989)**)
64. Ma, Y., Hu, K., Hu, X., Xu, J.: Robust preconditioners for incompressible MHD models. J. Comput. Phys. **316**, 721–746 (2016). https://doi.org/10.1016/j.jcp.2016.04.019
65. Girault, V., Raviart, P.-A.: Finite Element Methods for Navier–Stokes Equations. Theory and Algorithms. Springer Series in Computational Mathematics, vol. 5, p. 374. Springer, Berlin (1986). https://doi.org/10.1007/978-3-642-61623-5
66. Kolev, T.V., Vassilevski, P.S.: Parallel auxillary space AMG solver for H(div) problems. SIAM J. Sci. Comput. **34**(6), 3079–3098 (2012). https://doi.org/10.1137/110859361
67. Abousleiman, Y., Cheng, A.H.-D., Cui, L., Detournay, E., Roegiers, J.-C.: Mandel's problem revisited. Géotechnique **46**(2), 187–195 (1996). https://doi.org/10.1680/geot.1996.46.2.187
68. Davis, T.A.: Algorithm 832: UMFPACK, an unsymmetric-pattern multifrontal method. ACM Trans. Math. Softw. **30**(2), 196–199 (2004). https://doi.org/10.1145/992200.992206
69. Davis, T.A.: A column pre-ordering strategy for the unsymmetric-pattern multifrontal method. ACM Trans. Math. Softw. **30**(2), 165–195 (2004). https://doi.org/10.1145/992200.992205
70. Davis, T.A., Duff, I.S.: An unsymmetric-pattern multifrontal method for sparse LU factorization. SIAM J. Matrix Anal. Appl. **18**(1), 140–158 (1997). https://doi.org/10.1137/S089547989424690

71. Davis, T.A., Duff, I.S.: A combined unifrontal/multifrontal method for unsymmetric sparse matrices. ACM Trans. Math. Softw. **25**(1), 1–19 (1999). https://doi.org/10.1145/305658.287640
72. Raviart, P.-A., Thomas, J.M.: A mixed finite element method for 2nd order elliptic problems. In: Mathematical Aspects of Finite Element Methods (Proc. Conf., Consiglio Naz. delle Ricerche (C.N.R.), Rome, 1975). Springer, Berlin, pp. 292–315606 (1977). https://doi.org/10.1007/BFb0064470
73. Nédélec, J.-C.: A new family of mixed finite elements in $\mathbb{R}^3$. Numer. Math. **50**(1), 57–81 (1986). https://doi.org/10.1007/BF01389668
74. Nédélec, J.-C.: Mixed finite elements in $\mathbb{R}^3$. Numer. Math. **35**(3), 315–341 (1980). https://doi.org/10.1007/BF01396415
75. Crouzeix, M., Raviart, P.-A.: Conforming and nonconforming finite element methods for solving the stationary Stokes equations I. Rev. Française Autom. Inf. Rech. Opér. Sér. Rouge **7**(R–3), 33–75 (1973). https://doi.org/10.1051/m2an/197307R300331
76. Falk, R.S.: Nonconforming finite element methods for the equations of linear elasticity. Math. Comput. **57**(196), 529–550 (1991). https://doi.org/10.2307/2938702
77. Falk, R.S., Morley, M.E.: Equivalence of finite element methods for problems in elasticity. SIAM J. Numer. Anal. **27**(6), 1486–1505 (1990). https://doi.org/10.1137/0727086
78. Hansbo, P., Larson, M.G.: Discontinuous Galerkin and the Crouzeix–Raviart element: application to elasticity. Math. Model. Numer. Anal. **37**(1), 63–72 (2003). https://doi.org/10.1051/m2an:2003020